
This is the **accepted version** of the article:

Bjorkman, Anne D.; Myers-Smith, Isla H.; Elmendorf, Sarah C.; [et al.]. «Plant functional trait change across a warming tundra biome». *Nature*, Vol. 562 (Oct. 2018), 57-62. DOI 10.1038/s41586-018-0563-7

This version is available at <https://ddd.uab.cat/record/218184>

under the terms of the  **CC BY** COPYRIGHT license

Plant functional trait change across a warming tundra biome

Anne D. Bjorkman^{1,2,3*}, Isla H. Myers-Smith², Sarah C. Elmendorf^{4,5}, Signe Normand^{1,6,7},
Nadja R uger^{8,9}, Pieter S.A. Beck¹⁰, Anne Blach-Overgaard^{1,7}, Daan Blok¹¹, J. Hans C.
Cornelissen¹², Bruce C. Forbes¹³, Damien Georges^{14,2}, Scott J. Goetz¹⁵, Kevin Guay¹⁶,
Gregory H.R. Henry¹⁷, Janneke HilleRisLambers¹⁸, Robert D. Hollister¹⁹, Dirk N. Karger²⁰,
Jens Kattge^{21,8}, Peter Manning³, Janet S. Prevey²², Christian Rixen²², Gabriela Schaepman-
Strub²³, Haydn J.D. Thomas², Mark Vellend²⁴, Martin Wilmking²⁵, Sonja Wipf²², Michele
Carbognani²⁶, Luise Hermanutz²⁷, Esther Levesque²⁸, Ulf Molau²⁹, Alessandro Petraglia²⁶,
Nadejda A. Soudzilovskaia³⁰, Marko Spasojevic³¹, Marcello Tomaselli²⁶, Tage Vowles³²,
Juha M. Alatalo³³, Heather Alexander³⁴, Alba Anadon-Rosell^{35,36}, Sandra Angers-Blondin²,
Mariska te Beest^{37,38}, Logan Berner¹⁵, Robert G. Bj rk³², Agata Buchwal^{39,40}, Allan Buras⁴¹,
Katie Christie⁴², Laura S Collier²⁷, Elisabeth J. Cooper⁴³, Stefan Dullinger⁴⁴, Bo Elberling⁴⁵,
Anu Eskelinen^{46,8,47}, Esther R. Frei^{17,20}, Maitane Iturrate Garcia²³, Oriol Grau^{48,49}, Paul
Grogan⁵⁰, Martin Hallinger⁵¹, Karen A. Harper⁵², Monique M.P.D. Heijmans⁵³, James
Hudson⁵⁴, Karl H lber⁴⁴, Colleen M. Iversen⁵⁵, Francesca Jaroszynska^{56,22}, Jill Johnstone⁵⁷,
Rasmus Halfdan Jorgensen⁵⁸, Elina Kaarlejarvi^{37,59}, Rebecca Klady⁶⁰, Sara Kuleza⁵⁷, Aino
Kulonen²², Laurent J. Lamarque²⁸, Trevor Lantz⁶¹, Chelsea J. Little^{23,62}, James David Mervyn
Speed⁶³, Anders Michelsen^{64,65}, Ann Milbau⁶⁶, Jacob Nabe-Nielsen⁶⁷, Sigrid Sch ler
Nielsen¹, Josep M. Ninot^{35,36}, Steve Oberbauer⁶⁸, Johan Olofsson³⁷, Vladimir G.
Onipchenko⁶⁹, Sabine B. Rumpf⁴⁴, Philipp Semenchuk⁴³, Rohan Shetti²⁵, Lorna E. Street²,
Katharine Suding⁴, Ken D. Tape⁷⁰, Andrew Trant⁷¹, Urs Treier¹, Jean-Pierre Tremblay⁷²,
Maxime Tremblay²⁸, Susanna Venn⁷³, Stef Weijers⁷⁴, Tara Zamin⁵⁰, Noemie Boulanger-
Lapointe¹⁷, William A. Gould⁷⁵, Dave Hik⁷⁶, Annika Hofgaard⁷⁷, Ingibj rg Svala J nsson^{78,79},
Janet Jorgenson⁸⁰, Julia Klein⁸¹, Borgthor Magnusson⁸², Craig Tweedie⁸³, Philip A.
Wookey⁸⁴, Michael Bahn⁸⁵, Benjamin Blonder^{86,87}, Peter van Bodegom⁸⁸, Benjamin Bond-
Lamberty⁸⁹, Giandiego Campetella⁹⁰, Bruno E.L. Cerabolini⁹¹, F. Stuart Chapin III⁹², Will
Cornwell⁹³, Joseph Craine⁹⁴, Matteo Dainese⁹⁵, Franciska T. de Vries⁹⁶, Sandra D az⁹⁷,
Brian J. Enquist^{98,99}, Walton Green¹⁰⁰, Ruben Milla¹⁰¹,  lo Niinemets¹⁰², Yusuke Onoda¹⁰³,
Jenny Ordonez¹⁰⁴, Wim A. Ozinga^{105,106}, Josep Penuelas^{107,49}, Hendrik Poorter¹⁰⁸, Peter
Poschold¹⁰⁹, Peter B. Reich^{110,111}, Brody Sandel¹¹², Brandon Schamp¹¹³, Serge
Sheremetev¹¹⁴, Evan Weiher¹¹⁵

1. Ecoinformatics and Biodiversity, Department of Bioscience, Aarhus University, Ny Munkegade 114-116, DK-8000 Aarhus C
2. School of GeoSciences, University of Edinburgh, Edinburgh EH9 3FF, UK
3. Senckenberg Gesellschaft f r Naturforschung, Biodiversity and Climate Research Centre (BiK-F), Senckenberganlage 25, Frankfurt, Germany
4. Department of Ecology and Evolutionary Biology, University of Colorado, Boulder, Colorado 80309 USA
5. National Ecological Observatory Network, 1685 38th St, Boulder, CO 80301, USA
6. Arctic Research Center, Department of Bioscience, Aarhus University, Ny Munkegade 114-116, DK-8000 Aarhus C
7. Center for Biodiversity Dynamic in a Changing World (BIOCHANGE), Department of Bioscience, Aarhus University, Ny Munkegade 114-116, DK-8000 Aarhus C
8. German Centre for Integrative Biodiversity Research (iDiv) Halle-Jena-Leipzig, Leipzig, Germany

- 48 9. Smithsonian Tropical Research Institute, Apartado 0843-03092, Balboa Ancón,
49 Panama
- 50 10. European Commission, Joint Research Centre, Directorate D - Sustainable Resources,
51 Bio-Economy Unit, Via Enrico Fermi 2749, 21027, Ispra, Italy
- 52 11. Department of Physical Geography and Ecosystem Science, Lund University, Lund S-
53 223 62, Sweden
- 54 12. Systems Ecology, Department of Ecological Science, Vrije Universiteit, Amsterdam,
55 The Netherlands
- 56 13. Arctic Centre, University of Lapland, FI-96101 Rovaniemi, Finland
- 57 14. International Agency for Research in Cancer, Lyon, France
- 58 15. Northern Arizona University, Flagstaff, Arizona, USA
- 59 16. Bigelow Laboratory for Ocean Sciences, East Boothbay, Maine, USA
- 60 17. Department of Geography, University of British Columbia, Vancouver, BC V6T 1Z4,
61 Canada
- 62 18. Biology Department, University of Washington, Seattle, USA, 98195-1800
- 63 19. Biology Department, Grand Valley State University, 1 Campus Drive, Allendale
64 Michigan USA
- 65 20. Swiss Federal Research Institute WSL, Zürcherstrasse 111, 8903 Birmensdorf,
66 Switzerland
- 67 21. Max Planck Institute for Biogeochemistry, Jena, Germany
- 68 22. WSL Institute for Snow and Avalanche Research SLF, 7260 Davos, Switzerland
- 69 23. Department of Evolutionary Biology and Environmental Studies, University of Zurich,
70 Zurich, Switzerland
- 71 24. Département de biologie, Université de Sherbrooke, Sherbrooke, Québec, Canada
72 J1K 2R1
- 73 25. Institute of Botany and Landscape Ecology, Greifswald University, Greifswald,
74 Germany
- 75 26. Department of Chemistry, Life Sciences and Environmental Sustainability, University of
76 Parma, Parco Area delle Scienze 11/A, I-43124 Parma, Italy
- 77 27. Department of Biology, Memorial University, St. John's, Newfoundland and Labrador,
78 Canada A1B3X9
- 79 28. Département des Sciences de l'environnement et Centre d'études nordiques,
80 Université du Québec à Trois-Rivières, Trois-Rivières, QC, G9A 5H7, Canada
- 81 29. Department of Biological and Environmental Sciences, University of Gothenburg,
82 Gothenburg, Sweden
- 83 30. Conservation Biology Department, Institute of Environmental Sciences, Leiden
84 University, The Netherlands
- 85 31. Department of Evolution, Ecology, and Organismal Biology, University of California
86 Riverside, Riverside, CA.
- 87 32. Department of Earth Sciences, University of Gothenburg, P.O. Box 460, SE-405 30
88 Gothenburg, Sweden
- 89 33. Department of Biological and Environmental Sciences, Qatar University, Qatar
- 90 34. Department of Forestry, Forest and Wildlife Research Center, Mississippi State
91 University, MS 39762
- 92 35. Department of Evolutionary Biology, Ecology and Environmental Sciences, University
93 of Barcelona, Av. Diagonal 643 E-08028 Barcelona
- 94 36. Biodiversity Research Institute, University of Barcelona, Av. Diagonal 643 E-08028
95 Barcelona

- 96 37. Department of Ecology and Environmental Science, Umeå University, Sweden
97 38. Department of Environmental Sciences, Copernicus Institute, Utrecht University, the
98 Netherlands
99 39. Adam Mickiewicz University, Institute of Geoecology and Geoinformation,
100 B.Krygowskiego 10, 61-680 Poznan, Poland
101 40. University of Alaska Anchorage, Department of Biological Sciences, 3151 Alumni
102 Loop, Anchorage, Alaska 99508, USA
103 41. Ecoclimatology, Technische Universität München, Hans-Carl-von-Carlowitz-Platz 2,
104 85354 Freising
105 42. The Alaska Department of Fish and Game, 333 Raspberry Road, Anchorage, Alaska
106 99518
107 43. Department of Arctic and Marine Biology, Faculty of Biosciences, Fisheries and
108 Economics, UiT- The Arctic University of Norway, NO-9037 Tromsø, Norway
109 44. Department of Botany and Biodiversity Research, University of Vienna, Rennweg 14,
110 A-1030 Vienna, Austria
111 45. Center for Permafrost (CENPERM), Department of Geosciences and Natural Resource
112 Management, University of Copenhagen, DK-1350 Copenhagen, Denmark
113 46. Department of Physiological Diversity, Helmholtz Center for Environmental Research -
114 UFZ, Permoserstrasse 15, Leipzig 04103, Germany
115 47. Department of Ecology, University of Oulu, 90014 University of Oulu, Finland
116 48. Global Ecology Unit, CREAM-CSIC-UAB, Bellaterra, Catalonia 08193, Spain
117 49. CREAM, Cerdanyola del Vallès, Catalonia 08193, Spain
118 50. Department of Biology, Queen's University, Kingston, ON, Canada
119 51. Biology Department, Swedish Agricultural University (SLU), Uppsala, Sweden
120 52. Biology Department, Saint Mary's University, Halifax, NS, Canada
121 53. Plant Ecology and Nature Conservation Group, Wageningen University & Research,
122 Wageningen, The Netherlands
123 54. British Columbia Public Service, Canada
124 55. Climate Change Science Institute and Environmental Sciences Division, Oak Ridge
125 National Laboratory, Oak Ridge, TN, USA 37831
126 56. Institute of Biological and Environmental Sciences, University of Aberdeen, Aberdeen,
127 AB24 3UU
128 57. Department of Biology, University of Saskatchewan, Saskatoon SK S7N 5E2 Canada
129 58. Department of Geosciences and Natural Resource Management, University of
130 Copenhagen, Denmark
131 59. Department of Biology, Vrije Universiteit Brussel (VUB), Belgium
132 60. Department of Forest Resources Management, Faculty of Forestry, University of
133 British Columbia, Vancouver, BC, Canada
134 61. School of Environmental Studies, University of Victoria, Victoria, BC, Canada
135 62. Department of Aquatic Ecology, Eawag: Swiss Federal Institute of Aquatic Science and
136 Technology, Dübendorf, Switzerland
137 63. NTNU University Museum, Norwegian University of Science and Technology, NO-7491
138 Trondheim, Norway
139 64. Department of Biology, University of Copenhagen, Universitetsparken 15, DK-2100
140 Copenhagen, Denmark
141 65. Center for Permafrost (CENPERM), University of Copenhagen, Oster Voldgade
142 10, DK-1350 Copenhagen, Denmark
143 66. Research Institute for Nature and Forest (INBO), Havenlaan 88, box 73, 1000 Brussels

- 144 67. Department of Bioscience, Aarhus University, Frederiksborgvej 399, DK-4000
145 Roskilde, Denmark
- 146 68. Department of Biological Sciences, Florida International University, Miami FL 33199
147 USA
- 148 69. Department of Geobotany, Lomonosov Moscow State University, Moscow 119234,
149 Russia
- 150 70. Institute of Northern Engineering, University of Alaska Fairbanks, USA
- 151 71. School of Environment, Resources and Sustainability, University of Waterloo,
152 Waterloo, Ontario, Canada N2L 3G1
- 153 72. Département de biologie, Centre d'études nordiques and Centre d'étude de la forêt,
154 Université Laval, QC, G1V 0A6, Canada
- 155 73. Centre for Integrative Ecology, School of Life and Environmental Sciences, Deakin
156 University, 221 Burwood Highway, Burwood, VIC, Australia 3125
- 157 74. Department of Geography, University of Bonn, Meckenheimer Allee 166, D-53115
158 Bonn, Germany
- 159 75. USDA Forest Service International Institute of Tropical Forestry, Río Piedras, Puerto
160 Rico
- 161 76. Department of Biological Sciences, University of Alberta, Edmonton, AB, T6G 2E9,
162 Canada
- 163 77. Norwegian Institute for Nature Research, PO Box 5685 Sluppen, NO-7485 Trondheim,
164 Norway
- 165 78. Faculty of Life and Environmental Sciences, University of Iceland, 101 Reykjavík,
166 Iceland
- 167 79. University Centre in Svalbard, N-9171 Longyearbyen, Norway
- 168 80. Arctic National Wildlife Refuge, U. S. Fish and Wildlife Service
- 169 81. Department of Ecosystem Science & Sustainability, Colorado State University,
170 Campus Delivery 1476, Fort Collins, CO 80523-1476 USA
- 171 82. Icelandic Institute of Natural History, Gardabaer, Iceland
- 172 83. University of Texas at El Paso, El Paso, Texas, USA
- 173 84. Biology and Environmental Sciences, Faculty of Natural Sciences, University of
174 Stirling, Stirling, FK9 4LA, Scotland, UK
- 175 85. Institute of Ecology, University of Innsbruck, Innsbruck, Austria
- 176 86. Environmental Change Institute, School of Geography and the Environment, South
177 Parks Road, University of Oxford, Oxford OX1 3QY, UK
- 178 87. Rocky Mountain Biological Laboratory, PO Box 519, Crested Butte, Colorado, 81224
179 USA
- 180 88. Institute of Environmental Sciences, Leiden University, 2333 CC Leiden, the
181 Netherlands
- 182 89. Joint Global Change Research Institute, Pacific Northwest National Laboratory,
183 College Park, MD, USA
- 184 90. School of Biosciences & Veterinary Medicine - Plant Diversity and Ecosystems
185 Management unit, University of Camerino, via Pontoni, 5 - 62032, Italy
- 186 91. DiSTA - University of Insubria, via Dunant 3, 21100 Varese, Italy
- 187 92. Institute of Arctic Biology, University of Alaska Fairbanks, Fairbanks, AK 99709, USA
- 188 93. School of Biological, Earth & Environmental Sciences, Ecology and Evolution
189 Research Centre, UNSW Australia, Sydney, NSW 2052, Australia
- 190 94. Jonah Ventures, Manhattan KS 66502, USA
- 191 95. Institute for Alpine Environment, Eurac Research, Bolzano, Italy

- 192 96. School of Earth and Environmental Sciences, The University of Manchester, UK
193 97. Instituto Multidisciplinario de Biología Vegetal (IMBIV), CONICET and FCEfyN,
194 Universidad Nacional de Córdoba, Casilla de Correo 495, 5000 Córdoba, Argentina
195 98. Department of Ecology and Evolutionary Biology, University of Arizona, Tucson,
196 Arizona 85719, USA
197 99. The Santa Fe Institute, 1399 Hyde Park Road, Santa Fe, New Mexico 87501, USA
198 100. Department of Organismic and Evolutionary Biology, Harvard University, 26 Oxford
199 Street, Cambridge, MA 02138 USA
200 101. Área de Biodiversidad y Conservación. Departamento de Biología, Geología, Física y
201 Química Inorgánica. Universidad Rey Juan Carlos, 28933 Móstoles (Madrid), Spain
202 102. Estonian University of Life Sciences, Kreutzwaldi 1, 51014 Tartu, Estonia
203 103. Graduate School of Agriculture, Kyoto University, Oiwake, Kitashirakawa, Kyoto, 606-
204 8502 Japan
205 104. World Agroforestry Centre - Latin America, Av. La Molina 1895, La Molina, Lima, Perú
206 105. Team Vegetation, Forest and Landscape ecology, Wageningen Environmental
207 Research (Alterra), P.O. Box 47, NL-6700 AA Wageningen, The Netherlands
208 106. Institute for Water and Wetland Research, Radboud University Nijmegen, 6500 GL
209 Nijmegen, The Netherlands
210 107. Global Ecology Unit CREAf-CSIC-UAB, Consejo Superior de Investigaciones
211 Científicas, Bellaterra, Catalonia 08193, Spain
212 108. Plant Sciences (IBG-2), Forschungszentrum Jülich GmbH, Jülich 52425, Germany
213 109. Ecology and Conservation Biology, Institute of Plant Sciences, University of
214 Regensburg, D-93040 Regensburg
215 110. Department of Forest Resources, University of Minnesota, St. Paul, MN 55108 USA
216 111. Hawkesbury Institute for the Environment, Western Sydney University, Penrith NSW
217 2751, Australia
218 112. Department of Biology, Santa Clara University, 500 El Camino Real, Santa Clara, CA,
219 95053 USA
220 113. Department of Biology, Algoma University, Sault Ste. Marie, Ontario, Canada
221 114. Komarov Botanical Institute, Prof. Popov Street 2, St Petersburg 197376, Russia
222 115. Department of Biology, University of Wisconsin - Eau Claire, Eau Claire, WI 54702,
223 USA

224
225 * corresponding author (anne.bjorkman@senckenberg.de)
226
227

228 **Summary paragraph**

229 The tundra is warming more rapidly than any other biome on Earth, and the potential
230 ramifications are far-reaching due to global-scale vegetation-climate feedbacks. A better
231 understanding of how environmental factors shape plant structure and function is critical to
232 predicting the consequences of environmental change for ecosystem functioning. Here, we
233 explore the biome-wide relationships between temperature, moisture, and seven key plant
234 functional traits both across space and over three decades of warming at 117 tundra
235 locations. Spatial temperature-trait relationships were generally strong but soil moisture had
236 a marked influence on the strength and direction of these relationships, highlighting the
237 potentially important influence of changes in water availability on future plant trait change.
238 Community height increased with warming across all sites over the past three decades, but
239 other traits lagged far behind predicted rates of change. Our findings highlight the challenge
240 of using space-for-time substitution to predict the functional consequences of future warming
241 and suggest that functions tied closely to plant height will experience the most rapid change.
242 Our results reveal the strength with which environmental factors shape biotic communities at
243 the coldest extremes of the planet and will enable improved projections of tundra functional
244 change with climate warming.

245

246 **Main text**

247 Rapid climate warming in Arctic and alpine regions is driving changes in the structure and
248 composition of tundra ecosystems^{1,2}, with potentially global consequences. Up to 50% of the
249 world's belowground carbon stocks are contained in permafrost soils³, and tundra regions
250 are expected to contribute the majority of warming-induced soil carbon loss over the next
251 century⁴. Plant traits strongly impact carbon cycling and energy balance, which can in turn
252 influence regional and global climates⁵⁻⁷. Traits related to the resource economics
253 spectrum⁸, such as specific leaf area, leaf nitrogen content, and leaf dry matter content,
254 affect primary productivity, litter decomposability, soil carbon storage, and nutrient
255 cycling^{5,6,9,10}, while size-related traits such as leaf area and plant height influence
256 aboveground carbon storage, albedo, and hydrology¹¹⁻¹³ (Extended Data Table 1).
257 Quantifying the link between the environment and plant functional traits is therefore critical to
258 understanding the consequences of climate change, but such studies rarely extend into the
259 tundra¹⁴⁻¹⁶. Thus, the full extent of the relationship between climate and plant traits in the
260 planet's coldest ecosystems has never been assessed, and the consequences of climate
261 warming for tundra functional change are largely unknown.

262

263 Here, we quantify for the first time the biome-wide relationships between temperature, soil
264 moisture, and key traits that represent the foundation of plant form and function¹⁷, using the

265 largest dataset of tundra plant traits ever assembled (56,048 measured trait observations;
266 Fig. 1a and Extended Data Fig. 1a, Table S1). We examine five continuously distributed
267 traits related to plant size (adult plant height and leaf area) and to resource economy
268 (specific leaf area (SLA), leaf nitrogen content (leaf N), and leaf dry matter content (LDMC)),
269 as well as two categorical traits related to community-level structure (woodiness) and leaf
270 phenology/lifespan (evergreenness). Intraspecific trait variability is thought to be especially
271 important where diversity is low or where species have wide geographic ranges¹⁸, as in the
272 tundra. Thus, we analyze two underlying components of biogeographic patterns in the five
273 continuous traits: intraspecific variability (phenotypic plasticity or genetic differences among
274 populations) and community-level variability (species turnover or shifts in species'
275 abundances over space). We ask: 1) How do plant traits vary with temperature and soil
276 moisture across the tundra biome? 2) What is the relative influence of intraspecific trait
277 variability (ITV) versus community-level trait variation (estimated as community-weighted
278 trait means, CWM) for spatial temperature-trait relationships? 3) Are spatial temperature-trait
279 relationships explained by among-site differences in species abundance or species turnover
280 (presence-absence)?

281

282 A major impetus for quantifying spatial temperature-trait relationships is to provide an
283 empirical basis for predicting the potential consequences of future warming¹⁹⁻²¹. Thus, we
284 also estimate realized rates of community-level trait change over time using nearly three
285 decades of vegetation survey data at 117 tundra sites (Fig. 1a, Table S2). Focusing on
286 interspecific trait variation, we ask: 4) How do changes in community traits over three
287 decades of ambient warming compare to predictions from spatial temperature-trait
288 relationships? We expect greater temporal trait change when spatial temperature-trait
289 relationships are a) strong, b) unlimited by moisture availability, and c) due primarily to
290 abundance shifts instead of species turnover, given that species turnover over time depends
291 on immigration and is likely to be slow²². Finally, because total realized trait change in
292 continuous traits is comprised of both community-level variation and intraspecific trait
293 variation (ITV), we estimated the *potential* contribution of ITV to overall trait change
294 (CWM+ITV) using the modeled intraspecific temperature-trait relationships described above
295 (see Methods and Extended Data Fig. 1b). For all analyses, we used a generalizable
296 Bayesian modeling approach, which allowed us to account for the hierarchical spatial,
297 temporal and taxonomic structure of the data as well as multiple sources of uncertainty.

298

299 *Environment-trait relationships across the tundra biome*

300 We found strong spatial associations between temperature and community height, SLA, and
301 LDMC (Fig. 2a, Extended Data Fig. 2, Table S3) across the 117 survey sites. Both height

302 and SLA increased with summer temperature, but the temperature-trait relationship for SLA
303 was much stronger at wet than at dry sites. LDMC was negatively related to temperature,
304 and more strongly so at wet than at dry sites. Community woodiness decreased with
305 temperature, but the ratio of evergreen to deciduous woody species increased with
306 temperature, particularly in dry sites (Extended Data Fig. 3). These spatial temperature-trait
307 relationships suggest that long-term climate warming should cause pronounced shifts toward
308 communities of taller plants with more resource-acquisitive leaves (high SLA and low
309 LDMC), particularly where soil moisture is high.

310

311 Our results reveal a substantial moderating influence of soil moisture on community traits
312 across spatial temperature gradients^{2,23}. Both leaf area and leaf N decreased with warmer
313 temperatures in dry sites but increased with warmer temperatures in wet sites (Fig. 2a,
314 Table S4). Soil moisture was important in explaining spatial variation in all seven traits
315 investigated here, even when temperature alone was not (e.g., leaf area; Fig. 2a and
316 Extended Data Figure 2), potentially reflecting physiological constraints related to heat
317 exchange or frost tolerance when water availability is low²⁴. Thus, future warming-driven
318 changes in traits and associated ecosystem functions (e.g. decomposability) will likely
319 depend on current soil moisture conditions at a site²³. Furthermore, future changes in water
320 availability (e.g., via changes in precipitation, snow melt timing, permafrost, and hydrology²⁵)
321 could cause substantial shifts in these traits and their associated functions irrespective of
322 warming.

323

324 We found consistent intraspecific temperature-trait relationships for all five continuous traits
325 (Fig. 2b, Table S5). Intraspecific plant height and leaf area showed strong positive
326 relationships with summer temperature (i.e., individuals were taller and had larger leaves in
327 warmer locations) while intraspecific LDMC, leaf N and SLA were related to winter but not
328 summer temperature (Extended Data Fig. 2). The differing responses of intraspecific trait
329 variation to summer versus winter temperatures may indicate that size-related traits better
330 reflect summer growth potential while resource economics traits reflect tolerance of cold-
331 stress. These results, although correlative, suggest that trait variation expressed at the
332 individual or population level is related to the growing environment and that warming will
333 likely lead to substantial intraspecific trait change in many traits. Thus, the potential for trait
334 change over time is underestimated by using species-level trait means alone. Future work is
335 needed to disentangle the role of plasticity and genetic differentiation in explaining the
336 observed intraspecific temperature-trait relationships²⁶, as this will also influence the rate of
337 future trait change²⁷. Trait measurements collected over time and under novel (experimental)

338 conditions, as yet unavailable, would enable more accurate predictions of future intraspecific
339 trait change.

340

341 Partitioning the underlying causes of community temperature-trait relationships revealed that
342 species turnover explained most of the variation in traits across space (Fig. 2c), suggesting
343 that dispersal and immigration processes will primarily govern the rate of ecosystem
344 responses to warming. Shifts in species' abundances and intraspecific trait variation
345 accounted for a relatively small part of the overall temperature-trait relationship across space
346 (Fig 2c). Furthermore, the local trait pool in the coldest tundra sites (mean summer
347 temperature < 3 °C) is constrained relative to the tundra as a whole for many traits
348 (Extended Data Fig. 4). Together, these results indicate that the magnitude of warming-
349 induced community trait shifts will be limited without the arrival of novel species from warmer
350 environments.

351

352 *Community trait change over time*

353 Plant height was the only trait for which the community weighted mean changed over the 27
354 years of monitoring; it increased rapidly at nearly every survey site (Fig. 3 a&b, Extended
355 Data Fig. 3, Table S6). Inter-annual variation in community height was sensitive to summer
356 temperature (Fig. 3c, Extended Data Fig. 2, Table S7), implying that increases in community
357 height are responding to warming. However, neither the total rate of temperature change nor
358 soil moisture predicted the total rate of CWM change in any trait (Extended Data Fig. 5,
359 Table S8). Incorporating potential intraspecific trait variation (ITV) doubled the average
360 estimate of plant height change over time (Fig. 3a and 4a, dashed lines). Because spatial
361 patterns in ITV can be due to both phenotypic plasticity and genetic differences among
362 populations, this is likely a maximum estimate of the ITV contribution, for example if
363 intraspecific temperature-trait relationships are due entirely to phenotypic plasticity. The
364 increase in community height observed here is consistent with previous findings of
365 increasing vegetation height in response to experimental warming at a subset of these
366 sites²⁸ and with studies showing increased shrub growth over time¹¹.

367

368 Increasing community height over time was due largely to species turnover (rather than
369 shifts in abundance of the resident species; Fig 3b) and was driven by the immigration of
370 taller species rather than the loss of shorter ones (Extended Data Fig. 6, Table S9). This
371 turnover could reflect the movement of tall species upward in latitude and elevation or from
372 local species pools in nearby warmer microclimates. The magnitude of temporal change was
373 comparable to that predicted from the spatial temperature-trait relationship (Fig. 4a, solid
374 lines), indicating that temporal change in plant height is not currently limited by immigration

375 rates. The importance of immigration in explaining community height change is surprising
376 given the relatively short study duration and long lifespan of tundra plants, but is nonetheless
377 consistent with a previous finding of shifts towards warm-associated species in tundra plant
378 communities^{20,29}. If the observed rate of trait change continues (e.g., if immigration were
379 unlimited), community height (excluding potential change due to ITV) could increase by 20-
380 60% by the end of the century, depending on carbon emission, warming and water
381 availability scenarios (Extended Data Fig. 7).

382

383 *Consequences & Implications*

384 Recent (observed) and future (predicted) changes in plant traits, particularly height, are likely
385 to have important implications for ecosystem functions and feedbacks involving soil
386 temperature^{30,31}, decomposition^{5,10}, and carbon cycling³², as the potential for soil carbon loss
387 is particularly great in high-latitude regions⁴. For example, increasing plant height could
388 offset warming-driven carbon loss via increased carbon storage due to woody litter
389 production⁵ or via reduced decomposition due to lower summer soil temperatures caused by
390 shading^{3,30,32} (negative feedbacks). Positive feedbacks are also possible if branches or
391 leaves above the snowpack reduce albedo^{11,12} or increase snow accumulation, leading to
392 warmer winter soil temperatures and increased decomposition rates^{3,11}. The balance of
393 these feedbacks and thus the net impact of trait change on carbon cycling may depend on
394 the interaction between warming and changes in snow distribution³³ and water availability³⁴,
395 which remain major unknowns in the tundra biome.

396

397 The lack of an observed temporal trend in SLA and LDMC despite strong temperature-trait
398 relationships over space highlights the limitations of using space-for-time substitution for
399 predicting short-term ecological change. This disconnect could reflect the influence of
400 unmeasured changes in water availability, e.g. due to local-scale variation in the timing of
401 snowmelt or hydrology, that counter or swamp the effect of static soil moisture estimates.
402 For example, we would not expect substantial changes in traits demonstrating a spatial
403 temperature x moisture interaction (LDMC, leaf area, leaf N, and SLA), even in wet sites, if
404 warming also leads to drier soils. Perhaps tellingly, plant height was the only continuous trait
405 for which a temperature x moisture interaction was not important, and was predicted to
406 increase across all areas of the tundra regardless of recent soil moisture trends (Fig. 4c&d).
407 Spatial-temporal disconnects could also reflect dispersal limitation of potential immigrants
408 (e.g., with low LDMC and high SLA), or establishment failure due to novel biotic (e.g.,
409 herbivore³⁵) or abiotic (e.g., photoperiod³⁶) conditions other than temperature to which
410 immigrants are maladapted^{22,36}. Furthermore, community responses to climate warming

411 could be constrained by soil properties (e.g., organic matter, mineralization) that themselves
412 respond slowly to warming²⁰.

413

414 The patterns in functional traits described here reveal the extent to which environmental
415 factors shape biotic communities in the tundra. Strong temperature- and moisture-related
416 spatial gradients in traits related to competitive ability (e.g., height) and resource capture and
417 retention (e.g., leaf nitrogen, SLA) reflect tradeoffs in plant ecological strategy^{9,37} from
418 benign (warm, wet) to extreme (cold, dry) conditions. Community-level trait syndromes, as
419 reflected in ordination axes, are also strongly related to both temperature and moisture,
420 suggesting that environmental drivers structure not only individual traits but also trait
421 combinations and thus lead to a limited number of successful functional strategies in some
422 environments (e.g., woody, low-SLA and low-leaf N communities in warm, dry sites;
423 Extended Data Fig. 8). Thus, warming may lead to a community-level shift toward more
424 acquisitive plant strategies³⁷ in wet tundra sites, but toward more conservative strategies in
425 drier sites as moisture becomes more limiting.

426

427 Earth system models are increasingly moving to incorporate trait-environment relationships,
428 as this can substantially improve estimates of ecosystem change³⁸⁻⁴⁰. Our results inform
429 these projections of future tundra functional change³⁸ by explicitly quantifying the link
430 between temperature, moisture, and key functional traits across the biome. In particular, our
431 study highlights the importance of accounting for future changes in water availability, as this
432 will likely influence both the magnitude and direction of change for many traits. In addition,
433 we demonstrate that spatial trait-environment relationships are driven largely by species
434 turnover, suggesting that modeling efforts must account for rates of species immigration
435 when predicting the speed of future functional shifts. The failure of many traits (e.g. specific
436 leaf area) to match expected rates of change suggests that space-for-time substitution alone
437 may inaccurately represent near-term ecosystem change. Nevertheless, the ubiquitous
438 increase in community plant height reveals that functional change is already occurring in
439 tundra ecosystems.

440

441 **References**

- 442 1. Post, E. *et al.* Ecological dynamics across the Arctic associated with recent climate
443 change. *Science* **325**, 1355–1358 (2009).
- 444 2. Elmendorf, S. C. *et al.* Plot-scale evidence of tundra vegetation change and links to
445 recent summer warming. *Nature Climate Change* **2**, 453–457 (2012).
- 446 3. Sistla, S. A. *et al.* Long-term warming restructures Arctic tundra without changing net
447 soil carbon storage. *Nature* **497**, 615–618 (2013).
- 448 4. Crowther, T. W. *et al.* Quantifying global soil carbon losses in response to warming.
449 *Nature* **540**, 104–108 (2016).
- 450 5. Cornelissen, J. H. C. *et al.* Global negative vegetation feedback to climate warming
451 responses of leaf litter decomposition rates in cold biomes. *Ecology Letters* **10**, 619–
452 627 (2007).
- 453 6. Lavorel, S. & Garnier, E. Predicting changes in community composition and
454 ecosystem functioning from plant traits: revisiting the Holy Grail. *Functional Ecology*
455 **16**, 545–556 (2002).
- 456 7. Pearson, R. G. *et al.* Shifts in Arctic vegetation and associated feedbacks under
457 climate change. *Nature Climate Change* **3**, 673–677 (2013).
- 458 8. Wright, I. J. *et al.* The worldwide leaf economics spectrum. *Nature* **428**, 821–827
459 (2004).
- 460 9. Díaz, S. *et al.* The plant traits that drive ecosystems: Evidence from three continents.
461 *Journal of Vegetation Science* **15**, 295–304 (2004).
- 462 10. Cornwell, W. K. *et al.* Plant species traits are the predominant control on litter
463 decomposition rates within biomes worldwide. *Ecology Letters* **11**, 1065–1071 (2008).
- 464 11. Myers-Smith, I. H. *et al.* Shrub expansion in tundra ecosystems: dynamics, impacts
465 and research priorities. *Environ. Res. Lett.* **6**, 045509 (2011).
- 466 12. Sturm, M. & Douglas, T. Changing snow and shrub conditions affect albedo with
467 global implications. *J. Geophys. Res.* **110**, G01004 (2005).
- 468 13. Callaghan, T. V. *et al.* Effects on the Function of Arctic Ecosystems in the Short- and
469 Long-Term Perspectives. *AMBIO* **33**, 448–458 (2004).
- 470 14. Moles, A. T. *et al.* Global patterns in plant height. *Journal of Ecology* **97**, 923–932
471 (2009).
- 472 15. Moles, A. T. *et al.* Global patterns in seed size. *Global Ecology and Biogeography* **16**,
473 109–116 (2007).
- 474 16. Reich, P. B. & Oleksyn, J. Global patterns of plant leaf N and P in relation to
475 temperature and latitude. *Proc. Natl. Acad. Sci. U.S.A.* **101**, 11001–11006 (2004).
- 476 17. Díaz, S. *et al.* The global spectrum of plant form and function. *Nature* **529**, 167–171
477 (2016).

- 478 18. Siefert, A. *et al.* A global meta-analysis of the relative extent of intraspecific trait
479 variation in plant communities. *Ecology Letters* **18**, 1406–1419 (2015).
- 480 19. McMahon, S. M. *et al.* Improving assessment and modelling of climate change
481 impacts on global terrestrial biodiversity. *Trends Ecol. Evol.* **26**, 249–259 (2011).
- 482 20. Elmendorf, S. C. *et al.* Experiment, monitoring, and gradient methods used to infer
483 climate change effects on plant communities yield consistent patterns. *Proc. Natl.*
484 *Acad. Sci. U.S.A.* **112**, 448–452 (2015).
- 485 21. De Frenne, P. *et al.* Latitudinal gradients as natural laboratories to infer species'
486 responses to temperature. *Journal of Ecology* **101**, 784–795 (2013).
- 487 22. Sandel, B. *et al.* Contrasting trait responses in plant communities to experimental and
488 geographic variation in precipitation. *New Phytologist* **188**, 565–575 (2010).
- 489 23. Ackerman, D., Griffin, D., Hobbie, S. E. & Finlay, J. C. Arctic shrub growth trajectories
490 differ across soil moisture levels. **23**, 4294–4302 (2017).
- 491 24. Wright, I. J. *et al.* Global climatic drivers of leaf size. *Science* **357**, 917–921 (2017).
- 492 25. Wrona, F. J. *et al.* Transitions in Arctic ecosystems: Ecological implications of a
493 changing hydrological regime. *Journal of Geophysical Research: Biogeosciences* **121**,
494 650–674 (2016).
- 495 26. Read, Q. D., Moorhead, L. C., Swenson, N. G., Bailey, J. K. & Sanders, N. J.
496 Convergent effects of elevation on functional leaf traits within and among species.
497 *Functional Ecology* **28**, (2014).
- 498 27. Albert, C. H., Grassein, F., Schurr, F. M., Vieilledent, G. & Violle, C. When and how
499 should intraspecific variability be considered in trait-based plant ecology?
500 *Perspectives in Plant Ecology, Evolution and Systematics* **13**, 217–225 (2011).
- 501 28. Elmendorf, S. C. *et al.* Global assessment of experimental climate warming on tundra
502 vegetation: heterogeneity over space and time. *Ecology Letters* **15**, 164–175 (2012).
- 503 29. Gottfried, M. *et al.* Continent-wide response of mountain vegetation to climate change.
504 *Nature Climate Change* **2**, 111–115 (2012).
- 505 30. Blok, D. *et al.* Shrub expansion may reduce summer permafrost thaw in Siberian
506 tundra. *Global Change Biology* **16**, 1296–1305 (2010).
- 507 31. Blok, D., Elberling, B. & Michelsen, A. Initial stages of tundra shrub litter
508 decomposition may be accelerated by deeper winter snow but slowed down by spring
509 warming. *Ecosystems* **19**, 155–169 (2016).
- 510 32. Cahoon, S. M. P., Sullivan, P. F., Shaver, G. R., Welker, J. M. & Post, E. Interactions
511 among shrub cover and the soil microclimate may determine future Arctic carbon
512 budgets. *Ecology Letters* **15**, 1415–1422 (2012).

- 513 33. Lawrence, D. M. & Swenson, S. C. Permafrost response to increasing Arctic shrub
514 abundance depends on the relative influence of shrubs on local soil cooling versus
515 large-scale climate warming. *Environ. Res. Lett.* **6**, 045504 (2011).
- 516 34. Christiansen, C. T. *et al.* Enhanced summer warming reduces fungal decomposer
517 diversity and litter mass loss more strongly in dry than in wet tundra. *Global Change*
518 *Biology* **23**, 406–420 (2017).
- 519 35. Kaarlejärvi, E., Eskelinen, A. & Olofsson, J. Herbivores rescue diversity in warming
520 tundra by modulating trait-dependent species losses and gains. *Nat Comms* **8**, 1–8
521 (2017).
- 522 36. Bjorkman, A. D., Vellend, M., Frei, E. R. & Henry, G. H. R. Climate adaptation is not
523 enough: warming does not facilitate success of southern tundra plant populations in
524 the high Arctic. *Global Change Biology* **23**, 1540–1551 (2017).
- 525 37. Reich, P. B. The world-wide ‘fast–slow’ plant economics spectrum: a traits manifesto.
526 *Journal of Ecology* **102**, 275–301 (2014).
- 527 38. Wullschleger, S. D. *et al.* Plant functional types in Earth system models: past
528 experiences and future directions for application of dynamic vegetation models in
529 high-latitude ecosystems. *Annals of Botany* **114**, 1–16 (2014).
- 530 39. Butler, E. E. *et al.* Mapping local and global variability in plant trait distributions. *Proc.*
531 *Natl. Acad. Sci. U.S.A.* **114**, E10937–E10946 (2017).
- 532 40. Reich, P. B., Rich, R. L., Lu, X., Wang, Y.-P. & Oleksyn, J. Biogeographic variation in
533 evergreen conifer needle longevity and impacts on boreal forest carbon cycle
534 projections. *Proceedings of the National Academy of Sciences* **111**, 13703–13708
535 (2014).
- 536

537 **Figure 1. Geographic distribution of trait and vegetation survey data and climatic**
538 **change over the study period. a.** Map of all 56,048 tundra trait records and 117 vegetation
539 survey sites. **b-c.** Climatic change across the period of monitoring at the 117 vegetation
540 survey sites, represented as mean winter (coldest quarter) and summer (warmest quarter)
541 temperature (**b**) and frost day frequency (**c**). The size of the colored points on the map
542 indicates the relative quantity of trait measurements (larger circles = more measurements of
543 that trait at a given location) and the color indicates which trait was measured. The black
544 stars indicate the vegetation survey sites used in the community trait analyses (most stars
545 represent multiple sites). Trait data were included for all species that occur in at least one
546 tundra vegetation survey site; thus, while not all species are unique to the tundra, all do
547 occur in the tundra. Temperature change and frost frequency change were estimated for the
548 interval over which sampling was conducted at each site plus the preceding four years in
549 order to best reflect the time window over which tundra plant communities respond to
550 temperature change^{20,29}.

551

552 **Figure 2. Strong spatial relationships in traits across temperature and soil moisture**
553 **gradients are primarily explained by species turnover. a,** Community-level (CWM)
554 variation in functional traits across space (N = 1520 plots within 117 sites within 72 regions)
555 as related to mean summer (warmest quarter) temperature and soil moisture, and **b,**
556 intraspecific variation (ITV) across space as related to summer temperature (note the log
557 scale for height and leaf area). **c,** Standardized effect sizes were estimated for all
558 temperature-trait relationships both across communities (CWM; solid bars) and within
559 species (ITV; striped bars). Effect sizes for CWM temperature-trait relationships were further
560 partitioned into the proportion of the effect driven solely by species turnover (light bars) and
561 abundance shifts (dark bars) over space. Dashed lines indicate the estimated total
562 temperature-trait relationship over space if intraspecific trait variability is also accounted for
563 (CWM: ITV). The contribution of ITV is estimated from the spatial temperature-trait
564 relationships modeled in (**b**). Soil moisture in (**a**) was modeled as continuous but is shown
565 predicted only at low and high values to improve visualization. Transparent ribbons in (**a**)
566 and (**b**) indicate 95% credible intervals for model mean predictions. Grey lines in (**b**)
567 represent intraspecific temperature-trait relationships for each species (height: N = 80
568 species, LDMC: N = 43, leaf area: N = 85, leaf N: N = 85, SLA: N = 108; N of observations
569 per trait shown in Table S1). In all panels, asterisks indicate that the 95% credible interval on
570 the slope of the temperature-trait relationship did not overlap zero. In panel (**a**), two asterisks
571 indicate that the temperature x soil moisture interaction term did not overlap zero. Winter
572 temperature – trait relationships are shown in Extended Data Fig. 2. Community woodiness
573 and evergreenness are shown in Extended Data Fig. 3.

574

575 **Figure 3. A tundra-wide increase in community height over time is related to warming.**

576 **a**, Observed community trait change per year (transformed units). Solid lines indicate the
577 distribution of community-weighted mean (CWM) model slopes (trait change per site) while
578 dashed lines indicate the community-weighted mean plus potential intraspecific trait variation
579 modelled from spatial temperature-trait relationships (CWM+ITV). Circles (CWM), triangles
580 (CWM+ITV) and error bars indicate the mean and 95% credible interval for the overall rate of
581 trait change across all sites (N = 4575 plot-years within 117 sites within 38 regions). The
582 vertical black dashed line indicates 0 (no change over time). **b**, Standardized effect sizes for
583 CWM change over time were further partitioned into the proportion of the effect driven solely
584 by species turnover (light bars) or shifts in abundance of resident species (dark bars) over
585 time. Dashed lines indicate the estimated total trait change over time if predicted
586 intraspecific trait variability is also included (CWM+ITV). Stars indicate that the 95% CI on
587 the mean hyperparameter for CWM trait change over time did not overlap zero. **c**,
588 Temperature sensitivity of each trait as related to summer temperature (i.e., correspondence
589 between interannual variation in CWM trait values and interannual variation in temperature).
590 Temperatures associated with each survey year were estimated as five-year means
591 (temperature of the survey year and four preceding years) because this interval has been
592 shown to be most relevant to vegetation change in tundra²⁰ and alpine²⁹ plant communities.
593 Circles represent the mean temperature sensitivity across all 117 sites, error bars are 95%
594 credible intervals on the mean. Changes in community woodiness and evergreenness are
595 shown in Extended Data Fig. 3.

596

597 **Figure 4. Community height increases in line with space-for-time predictions but**

598 **other traits lag. a**, Observed community (CWM) trait change over time (colored lines)
599 across all 117 sites vs. expected CWM change over the duration of vegetation monitoring
600 (1989-2015) based on the spatial temperature-trait (CWM) relationship and the average rate
601 of recent summer warming across all sites (solid black lines). Colored dashed lines indicate
602 the estimated total change over time if predicted intraspecific trait variability is also included
603 (CWM+ITV). Values on the y-axis represent the magnitude of change relative to 0 (i.e., trait
604 anomaly), with 0 representing the trait value at t_0 . **b-c**, Total recent temperature change (**b**)
605 and soil moisture change (**c**) across the Arctic tundra (1979-2016). Temperature change
606 estimates are derived from CRU gridded temperature data, soil moisture change estimates
607 are derived from downscaled ERA-Interim soil moisture data. Circles in (**b**) represent the
608 sensitivity (cm per °C) of CWM plant height to summer temperature at each site (see Fig.
609 3c). Areas of high temperature sensitivity are expected to experience the greatest increases
610 in height with warming. **d-e**, Spatial trait-temperature-moisture relationships (Fig. 2a) were

611 used to predict total changes in height (**d**) and leaf N (**e**) over the entire 1979-2016 period
612 based on concurrent changes in temperature and soil moisture. Note that (**d**) and (**e**) reflect
613 the magnitude of *expected* change between 1979 and 2016, not observed trait change. See
614 methods for details of temperature change and soil moisture change estimates. The outline
615 of Arctic areas is based on the Circumpolar Arctic Vegetation Map
616 (<http://www.geobotany.uaf.edu/cavm>).

617

618 **Acknowledgements**

619 This paper is an outcome of the sTundra working group supported by sDiv, the Synthesis
620 Centre of the German Centre for Integrative Biodiversity Research (iDiv) Halle-Jena-Leipzig
621 (DFG FZT 118). ADB was supported by an iDiv postdoctoral fellowship and The Danish
622 Council for Independent Research - Natural Sciences (DFF 4181-00565 to SN). ADB, IHM-
623 S, HJDT and SA-B were funded by the UK Natural Environment Research Council
624 (ShrubTundra Project NE/M016323/1 to IHM-S) and SN by the Villum Foundation's Young
625 Investigator Programme (VKR023456). NR was supported by the DFG-Forschungszentrum
626 'German Centre for Integrative Biodiversity Research (iDiv) Halle-Jena-Leipzig' and
627 Deutsche Forschungsgemeinschaft DFG (RU 1536/3-1). AB was supported by EU-F7P
628 INTERACT (262693) and MOBILITY PLUS (1072/MOB/2013/0). ABO and SSN were
629 supported by the Danish Council for Independent Research - Natural Sciences (DFF 4181-
630 00565 to SN) and the Villum Foundation (VKR023456 to SN). SSN was additionally
631 supported by the Carlsberg Foundation (2013-01-0825). JMA was supported by the Carl
632 Tryggers stiftelse för vetenskaplig forskning, AH by the Research Council of Norway
633 (244557/E50), BE by the Danish National Research Foundation (CENPERM DNRF100), BM
634 by the Soil Conservation Service of Iceland, and ERF by the Swiss National Science
635 Foundation (#155554). BCF was supported by the Academy of Finland (256991) and JPI
636 Climate (291581). BJE was supported by an NSF ATB, CAREER, and Macrosystems
637 award. CMI was supported by the Office of Biological and Environmental Research in the
638 U.S. Department of Energy's Office of Science as part of the Next-Generation Ecosystem
639 Experiments in the Arctic (NGEE Arctic) project. DB was supported by The Swedish
640 Research Council (2015-00465) and Marie Skłodowska Curie Actions co-funding (INCA
641 600398). EW was supported by the National Science Foundation (DEB-0415383), UWEC -
642 ORSP, and UWEC - BCDT. GS-S and MIG were supported by the University of Zurich
643 Research Priority Program on Global Change and Biodiversity. HA was supported by NSF
644 PLR (1623764, 1304040). ISJ was supported by the Icelandic Research Fund (70255021)
645 and the University of Iceland Research Fund. JDMS was supported by the Research Council
646 of Norway (262064). JSP was supported by the U. S. Fish and Wildlife Service. JCO was
647 supported by Klimaat voor ruimte, Dutch national research program Climate Change and

648 Spatial Planning. J. Johnstone, PG, GHRH, NB-L, KAH, LSC and TZ were supported by the
649 Natural Sciences and Engineering Research Council of Canada (NSERC). GHRH, NB-L,
650 LSC and LH were supported by ArcticNet. GHRH, NB-L and LSC were supported by the
651 Northern Scientific Training Program. GHRH and NB-L were additionally supported by the
652 Polar Continental Shelf Program. NB-L was additionally supported by the Fonds de
653 recherche du Quebec: Nature et technologies and the Centre d'études Nordiques. JP was
654 supported by the European Research Council Synergy grant SyG-2013-610028
655 IMBALANCE-P. AAR, OG and JMN were supported by the Spanish OAPN (project
656 534S/2012) and European INTERACT project (262693 Transnational Access). KDT was
657 supported by NSF ANS-1418123. LS and PAW were supported by the UK Natural
658 Environment Research Council Arctic Terrestrial Ecology Special Topic Programme and
659 Arctic Programme (NE/K000284/1 to PAW). PAW was additionally supported by the
660 European Union 4th Environment and Climate Framework Programme (Project Number
661 ENV4-CT970586). MW was supported by DFG RTG 2010. RDH was supported by the US
662 National Science Foundation. SJG was supported by NASA NNX15AU03A. HJDT was
663 funded by a NERC doctoral training partnership grant (NE/L002558/1). VGO was supported
664 by the Russian Science Foundation (#14-50-00029). LB was supported by NSF ANS
665 (1661723) and SJG by NASA ABoVE (NNX17AE44G). BB-L was supported as part of the
666 Energy Exascale Earth System Model (E3SM) project, funded by the U.S. Department of
667 Energy, Office of Science, Office of Biological and Environmental Research. AE was
668 supported by the Academy of Finland (projects 253385 and 297191). The study has been
669 supported by the TRY initiative on plant traits (<http://www.try-db.org>), which is hosted at the
670 Max Planck Institute for Biogeochemistry, Jena, Germany and is currently supported by
671 DIVERSITAS/Future Earth and the German Centre for Integrative Biodiversity Research
672 (iDiv) Halle-Jena-Leipzig. ADB and SCE thank the US National Science Foundation for
673 support to receive training in Bayesian methods (grant # 1145200 to N. Thompson Hobbs).
674 The authors thank Helge Bruelheide and Julian Ramirez-Villegas for helpful input at earlier
675 stages of this project. We acknowledge the contributions of Steven Mamet, Mélanie Jean,
676 Kirsten Allen, Nathan Young, Jenny Lowe, Olof Eriksson, and many others to trait and
677 community composition data collection, and thank the governments, parks, field stations and
678 local and indigenous people for the opportunity to conduct research on their land.

679

680 **Author contributions**

681 ADB, IHM-S and SCE conceived the study, with input from the sTundra working group (SN,
682 NR, PSAB, AB-O, DB, JHCC, WC, BCF, DG, SJG, KG, GHRH, RDH, JK, JSP, JHRL, CR,
683 GS-S, HJDT, MV, MW, and SW). ADB performed the analyses, with input from IHM-S, NR,
684 SCE, and SN. DNK made the maps of temperature, moisture, and trait change. ADB wrote

685 the manuscript, with input from IHM-S, SCE, SN, NR, and contributions from all authors.
686 ADB compiled the Tundra Trait Team database, with assistance from IHM-S, HJDT and SA-
687 B. Authorship order was determined as follows: 1) core authors, 2) sTundra participants
688 (alphabetical) and other major contributors, 3) authors contributing both trait (Tundra Trait
689 Team) and community composition (ITEX, etc.) data (alphabetical), 4) Tundra Trait Team
690 contributors (alphabetical), 5) community composition data only contributors (alphabetical),
691 and 6) TRY trait data contributors (alphabetical).

692

693 **Author Information**

694

695 Reprints and permissions information is available at www.nature.com/reprints.

696

697 The authors declare no competing financial interests.

698

699 Correspondence and requests for materials should be addressed to

700 anne.bjorkman@senckenberg.de.

701

702 **METHODS**

703

704 Below we describe the data, workflow (Extended Data Fig. 1b) and detailed methods used to
705 conduct all analyses.

706

707 **COMMUNITY COMPOSITION DATA**

708 Community composition data used for calculating community-weighted trait means were
709 compiled from a previous synthesis of tundra vegetation resurveys² (including many
710 International Tundra Experiment (ITEX) sites) and expanded with additional sites (e.g.,
711 Gavia Pass in the Italian Alps and three sites in Sweden) and years (e.g., 2015 survey data
712 added for Iceland sites, QHI, and Alexandra Fiord; Table S2). We included only sites for
713 which community composition data were roughly equivalent to percent cover (i.e., excluding
714 estimates approximating biomass), for a total of 117 sites (defined as plots in a single
715 contiguous vegetation type) within 38 regions (defined as a CRU⁴¹ grid cell). Plot-level
716 surveys of species composition and cover were conducted at each of these sites between
717 1989 and 2015 (see² for more details of data collection and processing). On average, there
718 were 15.2 plots per site. Repeat surveys were conducted over a minimum duration of 5 and
719 up to 21 years between 1989 and 2015 (mean duration = 13.6 years), for a total of 1,781
720 unique plots and 5,507 plot-year combinations. Plots were either permanent (i.e., staked;
721 62% of sites) or semi-permanent (38%), such that the approximate but not exact location
722 was resurveyed. The vegetation monitoring sites were located in tree-less Arctic or alpine
723 tundra and ranged in latitude from 40° (Colorado Rockies) to 80° (Ellesmere Island, Canada)
724 and were circumpolar in distribution (Fig. 1a, Table S2). Our analyses only include vascular
725 plants because there was insufficient trait data for non-vascular species. Changes in
726 bryophytes and other cryptogams are an important part of the trait and function change in
727 tundra ecosystems^{42,43}, thus the incorporation of non-vascular plants and their traits is a
728 future research priority.

729

730 *Temperature extraction for community composition observations*

731 We extracted summer (warmest quarter) and winter (coldest quarter) temperature estimates
732 for each of the vegetation survey sites from both the WorldClim⁴⁴ (for long-term averages;
733 <http://www.worldclim.org/>) and CRU⁴¹ (for temporal trends; <http://www.cru.uea.ac.uk/>)
734 gridded climate datasets. WorldClim temperatures were further corrected for elevation
735 (based on the difference between the recorded elevation of a site and the mean elevation of
736 the WorldClim grid cell) according to a correction factor of -0.005 °C per meter increase in
737 elevation. This correction factor was calculated by extracting the mean temperature and
738 elevation (WorldClim 30s resolution maps) of all cells falling in a 2.5 km radius buffer around

739 our sites and fitting a linear mixed model (with site as a random effect) to estimate the rate of
740 temperature change with elevation.

741

742 The average long-term (1960-present) temperature trend across all sites was 0.26 (range -
743 0.06 to 0.49) and 0.43 (range -0.15 to 1.32) °C/decade for summer and winter temperature,
744 respectively.

745

746 *Soil moisture for community composition observations*

747 A categorical measure of soil moisture at each site was provided by every site PI according
748 to the methods described in Elmendorf et al. 2012 and Myers-Smith et al. 2015 ^(2,45). Soil
749 moisture was considered to be 1) dry when during the warmest month of the year the top 2
750 cm of the soil was dry to the touch, 2) moist when soils were moist year round, but standing
751 water was not present, and 3) wet when standing water was present during the warmest
752 month of the year.

753

754 *Soil moisture change for maps of environmental and trait change (Fig. 4b-e)*

755 We used high-resolution soil moisture observations from ESA CCI SM v04.2. To calculate
756 the mean distribution of soil moisture, we averaged the observations from 1979-2016.
757 Because the ESA CCI SM temporal coverage is poor for our sites, temporal data were
758 instead taken from ERA-Interim (Volumetric soil water layer 1) for the same time period. We
759 downscaled the ERA-Interim data to the 0.05° resolution of ESA CCI SM v04.2 using
760 climatologically aided interpolation (delta change method)⁴⁶. The change in soil water
761 content was then calculated separately for each grid cell using linear regression with month
762 as a predictor variable. To classify the soil moisture data into three categories (wet, mesic,
763 dry) to match the community composition dataset, we used a quantile approach on the mean
764 soil moisture within the extent of the Arctic. We assigned the lowest quantile to dry and the
765 highest to wet conditions. For the trends in soil moisture between 1979-2016 we calculated
766 the percentage in change in relation to the mean first, and then calculated the change based
767 on the categorical data (e.g. 5% change from category 1 (dry) to category 2 (mesic)).

768

769 *Changes in water availability for analysis*

770 Although the strong effect of soil moisture on spatial temperature-trait relationships suggests
771 that change in water availability over time will play an important role in mediating trait
772 change, we did not use the CRU estimates of precipitation change over time because of
773 issues with precipitation records at high latitudes and the inability of gridded datasets to
774 capture localized precipitation patterns (e.g., ^{47,48}). The CRU precipitation trends at our sites
775 included many data gaps filled by long-term mean values, especially at the high-latitude

776 sites⁴⁵. As a purely exploratory analysis, we used the downscaled ERA-Interim data
777 described above to investigate whether trait change is related to summer soil moisture
778 change (June, July, and August; Extended Data Fig. 5b). However, we caution that soil
779 moisture change in our tundra sites is primarily controlled by snow melt timing, soil drainage,
780 the permafrost table and local hydrology²⁵, and as such precipitation records and coarse-
781 grain remotely sensed soil moisture change data are unlikely to accurately represent local
782 changes in soil water availability. For this same reason we did not use the ERA-Interim data
783 to explore spatial relationships between temperature, moisture and community traits, as the
784 categorical soil moisture data (described above) were collected specifically within each
785 community composition site and are therefore a more accurate representation of long-term
786 mean soil moisture conditions in that specific location.

787

788 **TRAIT DATA**

789 Continuous trait data (adult plant height, leaf area (average one-sided area of a single leaf),
790 specific leaf area (leaf area per unit of leaf dry mass; SLA), leaf nitrogen content (per unit of
791 leaf dry mass; leaf N), and leaf dry matter content (leaf dry mass per unit of leaf fresh mass;
792 LDMC); Fig. 1a & Extended Data Fig. 1a, Table S1) were extracted from the TRY⁴⁹ 3.0
793 database (available at www.try-db.org). We also ran a field & data campaign in 2014-15 to
794 collect additional in-situ tundra trait data (the “Tundra Trait Team” (TTT) dataset⁵⁰) to
795 supplement existing TRY records. All species names from the vegetation monitoring sites,
796 TRY and TTT were matched to accepted names in The Plant List using the R package
797 Taxonstand⁵¹ (v. 1.8) before merging the datasets. Community-level traits (woodiness and
798 evergreenness) were derived from functional group classifications for each species².
799 Woodiness is estimated as the proportion (abundance) of woody species in the plot, while
800 evergreenness is the proportion of evergreen woody species abundance out of all woody
801 species (evergreen plus deciduous) in a plot. Because some sites did not contain any woody
802 species (and thus the proportion of evergreen woody species could not be calculated), this
803 trait is estimated only for 98 of the 117 total sites.

804

805 *Data cleaning - TRY*

806 TRY trait data were subjected to a multi-step cleaning process. First, all values that did not
807 represent individual measurements or approximate species means were excluded. When a
808 dataset within TRY contained only coarse plant height estimates (e.g., estimated to the
809 nearest foot), we removed these values unless no other estimate of height for that species
810 was available. We then identified overlapping datasets within TRY and removed duplicate
811 observations whenever possible. The following datasets were identified as having partially
812 overlapping observations: GLOPNET – Global Plant Trait Network Database, The LEDA

813 Traitbase, Abisko & Sheffield Database, Tundra Plant Traits Database, and KEW Seed
814 Information Database (SID).

815

816 We then removed duplicates within each TRY dataset (e.g., if a value is listed once as
817 “mean” and again as “best estimate”) by first calculating the ratio of duplicated values within
818 each dataset, and then removing duplicates from datasets with more than 30% duplicated
819 values. This cutoff was determined by manual evaluation of datasets at a range of
820 thresholds. Datasets with fewer than 30% duplicated values were not cleaned in this way as
821 any internally duplicate values were assumed to be true duplicates (i.e., two different
822 individuals were measured and happened to have the same measurement value).

823

824 We also removed all species mean observations from the “Niwot Alpine Plant Traits”
825 database and replaced it with the original individual observations as provided by M.J.
826 Spasojevic.

827

828 *Data cleaning – TRY & TTT combined*

829 Both datasets were checked for improbable values, with the goal of excluding likely errors or
830 measurements with incorrect units but without excluding true extreme values. We followed a
831 series of data-cleaning steps, in each case identifying whether a given observation (x) was
832 likely to be erroneous (i.e. “error risk”) by calculating the difference between x and the mean
833 (excluding x) of the taxon and then dividing by the standard deviation of the taxon.

834

835 We employed a hierarchical data cleaning method, because the standard deviation of a trait
836 value is related to the mean and sample size. First, we checked individual records against
837 the entire distribution of observations of that trait and removed any records with an error risk
838 greater than 8 (i.e., a value more than 8 standard deviations away from the trait mean). For
839 species that occurred in four or more unique datasets with TRY or TTT (i.e., different data
840 contributors), we estimated a species mean per dataset and removed observations for which
841 the species mean error risk was greater than 3 (i.e., the species mean of that dataset was
842 more than 3 SD’s away from the species mean across all datasets). For species that
843 occurred in fewer than 4 unique datasets, we estimated a genus mean per dataset and
844 removed observations in datasets for which the error risk based on the genus mean was
845 greater than 3.5. Finally, we compared individual records directly to the distribution of values
846 for that species. For species with more than 4 records, we excluded values above an error
847 risk Y, where Y was dependent on the number of records of that species and ranged from an
848 error risk of 2.25 for species with fewer than 10 records to an error risk of 4 for species with
849 more than 30 records. For species with four or fewer records, we manually checked trait

850 values and excluded only those that were obviously erroneous, based on our expert
851 knowledge of these species.

852

853 This procedure was performed on the complete tundra trait database – including species
854 and traits not presented here. In total 2,056 observations (1.6%) were removed. In all cases,
855 we visually checked the excluded values against the distribution of all observations for each
856 species to ensure that our trait cleaning protocol was reasonable.

857

858 Trait data were distributed across latitudes within the tundra biome (Extended Data Fig. 1a).
859 All trait observations with latitude/longitude information were mapped and checked for
860 implausible values (e.g., falling in the ocean). These values were corrected from the original
861 publications or by contacting the data contributor whenever possible.

862

863 *Final trait database*

864 After cleaning out duplicates and outliers as described above, we retained 56,048 unique
865 trait observations (of which 18,613 are contained in TRY and 37,435 were newly contributed
866 by the Tundra Trait Team⁵⁰ field campaign) across the five traits of interest. Of the 447
867 identified species in the ITEX dataset, 386 (86%) had trait data available from TRY or TTT
868 for at least one trait (range 52-100% per site). Those species without trait data generally
869 represent rare or uncommon species unique to each site; on average, trait data were
870 available for 97% of total plant cover across all sites (range 39-100% per site; Table S1).

871

872 *Temperature extraction for trait observations*

873 WorldClim climate variables were extracted for all trait observations with latitude/longitude
874 values recorded (53,123 records in total, of which 12,380 were from TRY and 33,621 from
875 TTT). Because most observations did not include information about elevation, temperature
876 estimates for individual trait observations were not corrected for elevation and thus represent
877 the temperature at the mean elevation of the WorldClim grid cell.

878

879 **ANALYSES**

880

881 *Terminology*

882 Here we provide a brief description of acronyms and symbols used in the methods and
883 model equations.

884

885 **ITV** – intraspecific trait variation: variation in trait values within the same species

886 **CWM** – community weighted trait mean: the mean trait value of all species in a plot,
887 weighted by their abundance in the plot
888 **CWM + ITV** – community weighted trait mean, adjusted with the estimated contribution of
889 intraspecific trait variation based on the intraspecific temperature-trait relationship of each
890 species
891 α – alpha, used to designate lower-level model intercepts
892 β – beta, used to designate lower-level model slopes
893 γ – gamma, used to designate the model parameters of interest (e.g. the temperature-trait
894 relationship)

895

896 **Models**

897 All analyses were conducted in JAGS and/or Stan through R (v. 3.3.3) using packages
898 *rjags*⁵² (v. 4.6) and *rstan*⁵³ (v. 2.14.1). In all cases, models were run until convergence was
899 reached, as assessed both visually in traceplots and by ensuring that all Gelman-Rubin
900 convergence diagnostic (Rhat⁵⁴) values were less than 1.1.

901

902 A major limitation of the species mean trait approach often employed in analyses of
903 environment-trait relationships has been the failure to account for intraspecific trait variation
904 (ITV) that could be as or more important than interspecific variation^{55,56}. We addressed this
905 issue by employing a hierarchical analysis that incorporates both within-species and
906 community-level trait variation across climate gradients to estimate trait change over space
907 and time at the biome scale. We used a Bayesian approach that accounts for the
908 hierarchical spatial (plots within sites within regions) and taxonomic (intra- and inter-specific
909 variation) structure of the data as well as uncertainty in estimated parameters introduced
910 through absences in trait records for some species, and taxa that were identified to genus or
911 functional group (rather than species) in vegetation surveys.

912

913 *Intraspecific trait variation*

914 We subsetting the trait dataset to just those species for which traits had been measured in at
915 least four unique locations spanning a temperature range of at least 10% of the entire
916 temperature range (2.6°C and 5.0 °C for summer and winter temperature, respectively), and
917 for which the latitude and longitude of the measured individual or group of individuals was
918 recorded. The number of species meeting these criteria varied by trait and temperature
919 variable: 108-109 for SLA, 80-86 for plant height, 74-72 for leaf nitrogen, 85-76 for leaf area,
920 and 43-52 for LDMC, for summer and winter temperature, respectively. These species
921 counts correspond to 53-73% of community abundance. The relationship between each trait
922 and temperature (Fig. 2b) was estimated from a Bayesian hierarchical model, with

923 temperature as the predictor variable and species (s) and dataset-by-location (d) modeled
924 as random effects:
925

$$\begin{aligned} \text{traitobs}_i &\sim \text{logNormal}(\alpha_{s,d}, \sigma_s) \\ \alpha_{s,d} &\sim \text{Normal}(\alpha_s + \beta_s \cdot \text{temperature}_d, \sigma_1) \\ \beta_s &\sim \text{Normal}(B, \sigma_2) \\ \alpha_s &\sim \text{Normal}(A, \sigma_3) \end{aligned}$$

926
927 where i represents each trait observation and A and B are the intercept and slope
928 hyperparameters, respectively. Because LDMC represents a ratio and is thus bound
929 between 0 and 1, we used a beta error distribution for this trait. Temperature values were
930 mean-centered within each species. We used non-informative priors for all coefficients.
931

932 We further explored whether the strength of intraspecific temperature-height relationships
933 varied by functional group. We find that all functional groups (including dwarf shrubs, which
934 are genetically limited in their ability to grow upright) show similar temperature-trait
935 relationships (Extended Data Fig. 9a). These results suggest that the intraspecific
936 temperature-trait relationships may not only be a response of individual growth changes, and
937 are not restricted to particular functional groups with greater capacity for vertical growth
938 (e.g., tall shrubs and graminoids versus dwarf shrubs and certain forb species).
939

940 *Calculation of community weighted mean (CWM) values*

941 We calculated the community-weighted trait mean (i.e., the mean trait value of all species in
942 a plot, weighted by the abundance of each species), for all plots within a site. We employed
943 a Bayesian approach to calculate trait means for every species (s) using an intercept-only
944 model (such that the intercept per species (α_s) is equivalent to the mean trait value of the
945 species) and variation per species (σ_s) with a lognormal error distribution.
946

$$\text{traitobs}_i \sim \text{logNormal}(\alpha_s, \sigma_s)$$

947
948 Because LDMC represents a ratio and is thus bound between 0 and 1, we used a beta error
949 distribution instead of lognormal for this trait. When a species was measured multiple times
950 in several different locations, we additionally included a random effect of dataset-by-location
951 (d) to reduce the influence of a single dataset with many observations at one site when
952 calculating the mean per species:
953

$$\text{traitobs}_i \sim \text{logNormal}(\alpha_{s,d}, \sigma_d)$$

$$\alpha_{s,d} \sim \text{Normal}(\alpha_s, \sigma_s)$$

954

955 We used non-informative priors for all species intercept parameters for which there were
956 four or more unique trait observations, so that the species-level intercept and variance
957 around the intercept per species were estimated from the data. In order to avoid removing
958 species with little or no trait data from the analyses, we additionally employed a “gap-filling”
959 approach that allowed us to estimate a species’ trait mean while accounting for uncertainty
960 in the estimation of this mean. For species with fewer than four but more than one trait
961 observation, we used a normal prior with the mean equal to the mean of the observation(s)
962 and variance estimated based on the mean mean-variance ratio across all species. In other
963 words, we calculated the ratio of mean trait values to the standard deviation of those trait
964 values per species for all species with greater than four observations, then took the mean of
965 these ratios across all species and multiplied this number by the mean of species X (where
966 X is a species with 1-4 observations) to get the prior for σ . For species with no observations
967 (see Table S1), we used a prior mean equal to the mean of all species in the same genus
968 and a prior variance estimated based on the mean mean-variance ratio of all species in that
969 genus or 1.5 times the mean, whichever was lower. If there were no other species in the
970 same genus, then we used a prior mean equal to the mean of all other species in the family
971 and a prior variance estimated based on the mean mean-variance ratio of all species in the
972 family or 1.5 times the mean, whichever was lower.

973

974 *Calculation of CWM values: incorporating uncertainty in species traits*

975 In order to include uncertainty about species trait means (due to intraspecific trait variation,
976 missing trait information for some species, or when taxa were identified to genus or
977 functional group rather than species) in subsequent analyses, we estimated community-level
978 trait values per plot by sampling from the posterior distribution (mean +/- SD) of each
979 species intercept estimate and multiplying this distribution by the relative abundance of each
980 species in the plot to get a community-weighted mean (CWM) distribution per plot (p):

981

$$\text{Normal}(\text{CWMmean}_p, \text{CWMsd}_p)$$

982

983 This approach generates a distribution of CWM values per plot that propagates the
984 uncertainty in each species’ trait mean estimate into the plot-level (CWM) estimate. By using
985 a Bayesian approach, we are able to carry through uncertainty in trait mean estimates to all

986 subsequent analyses and reduce the potential for biased or deceptively precise estimates
987 due to missing trait observations.

988

989 *Calculation of CWM values: partitioning turnover and estimating contribution of ITV*

990 To assess the degree to which the spatial temperature-trait relationships are caused by
991 species turnover versus shifts in abundance among sites, we repeated each analysis using
992 the non-weighted community mean (all species weighted equally) of each plot. Temperature-
993 trait relationships estimated with non-weighted community means are due solely to species
994 turnover across sites. Finally, we assessed the potential contribution of intraspecific trait
995 variation (ITV) to the community-level temperature-trait relationship by using the modeled
996 intraspecific temperature-trait relationship (described above) to predict trait “anomaly” values
997 for each species at each site based on the temperature of that site in a given year relative to
998 its long-term average.

999

1000 An intraspecific temperature-trait relationship could not be estimated for every species due
1001 to an insufficient number of observations for some species. Therefore, we used the mean
1002 intraspecific temperature-trait slope across all species to predict trait anomalies for species
1003 without intraspecific temperature-trait relationships. These site- and year-specific species
1004 trait estimates were then used to calculate “ITV-adjusted” community-weighted means
1005 (CWM+ITV) for each plot in each year measured, and modeled as for CWM alone. As these
1006 “adjusted” values are estimated *relative to each species’ mean value*, the spatial
1007 temperature-trait relationship that includes this adjustment does not remove any bias in the
1008 underlying species mean data. For example, if southern tundra species tend to be measured
1009 at the southern edge of their range while northern tundra species tend to be measured at the
1010 northern edge of their range, the overall spatial temperature-trait relationship could appear
1011 stronger than it really is for species with temperature-related intraspecific variation. This is a
1012 limitation of any species-mean approach.

1013

1014 Estimates of temporal CWM+ITV temperature-trait relationships are not prone to this same
1015 limitation as they represent relative change, but should also be interpreted with caution as
1016 intraspecific temperature-trait relationships may be due to genetic differences among
1017 populations rather than plasticity, thus suggesting that trait change would not occur
1018 immediately with warming. We therefore caution that the CWM+ITV analyses presented
1019 here represent estimates of the potential contribution of ITV to overall CWM temperature-
1020 trait relationships over space and time, but should not be interpreted as measured
1021 responses.

1022

1023 In sum, we incorporate intraspecific variation into our analyses in three ways. First, by using
1024 the posterior distribution (rather than a single mean value) of species trait mean estimates in
1025 our calculations of CWM values per plot, so that information about the amount of variation
1026 within species is incorporated into all the analyses in our study. Second, by explicitly
1027 estimating intraspecific temperature-trait relationships based on the spatial variation in
1028 individual trait observations. And finally, by using these modeled temperature-trait
1029 relationships to inform estimates of the potential contribution of ITV to overall (CWM+ITV)
1030 temperature-trait relationships over space and time.

1031

1032 *Spatial community trait models (Fig. 2 a&c)*

1033 To investigate spatial relationships in plant traits with summer and winter temperature and
1034 soil moisture we used a Bayesian hierarchical modeling approach in which soil moisture and
1035 soil moisture x temperature vary at the site level while temperature varies by WorldClim
1036 region (unique WorldClim grid x elevation groups). In total, there were 117 sites (s) nested
1037 within 73 WorldClim regions (r). We used only the first year of survey data at each site to
1038 estimate spatial relationships in community traits.

1039

$$\begin{aligned}CWMmean_p &\sim Normal(\alpha_s + \alpha_r, CWMsd_p) \\ \alpha_s &\sim Normal(\gamma_1 \cdot moisture_s + \gamma_2 \cdot moisture_s \cdot temperature_s, \sigma_1) \\ \alpha_r &\sim Normal(\gamma_0 + \gamma_3 \cdot temperature_r, \sigma_2)\end{aligned}$$

1040

1041 Where $CWMmean_p$ is the mean of the posterior distribution of the community-weighted
1042 mean (CWM) estimate per plot (p) and $CWMsd_p$ is the standard deviation of the posterior
1043 distribution of the CWM estimate per plot, as described in the “*Calculation of CWM values:
1044 incorporating uncertainty in species traits*” section. See supplementary information for
1045 complete STAN code.

1046

1047 As woodiness and evergreenness represent proportional data (bounded between 0 and 1,
1048 inclusive), we used a beta-Bernoulli mixture model of the same structure as above to
1049 estimate trait-temperature-moisture relationships for these traits (Extended Data Fig. 3 a&b).
1050 The discrete and continuous components of the data were modeled separately, with mixing
1051 occurring at the site- and region-level estimates (α_s and α_r).

1052

1053 Because Arctic and alpine tundra sites might differ in their trait-environment relationships
1054 due to environmental differences in e.g. soil drainage, we also performed a version of the
1055 spatial community trait analyses in which the elevation of each site is visually indicated (not

1056 modeled; Extended Data Fig. 9b). We did not attempt to separately analyze trait-
1057 environment relationships for Arctic and alpine sites due to the ambiguity in defining this cut-
1058 off (i.e., many sites can be categorized as both Arctic and alpine, particularly in Scandinavia
1059 and Iceland) and because of the small number of southern, high-alpine sites (European Alps
1060 and Colorado Rockies).

1061

1062 For estimation of the overall temperature-trait relationship, we used a model structure similar
1063 to that above but with only temperature as a predictor (i.e., without soil moisture). This model
1064 was used for both community-weighted mean (CWM) and non-weighted mean estimates in
1065 order to determine the degree to which temperature-trait relationships over space are due to
1066 species turnover alone (non-weighted mean) and for CWM+ITV plot-level estimates to
1067 determine the likely additional contribution of intraspecific trait variation to the overall
1068 temperature-trait relationship, as described above.

1069

1070 Standardized effect sizes for CWM temperature-trait relationships (Fig. 2c) were obtained by
1071 dividing the slope of the temperature-trait relationship by the standard deviation of the CWM
1072 model residuals. Effect sizes for ITV, turnover only, and CWM: ITV were estimated relative
1073 to the CWM value for that same trait based on the slope values of each temperature-trait
1074 relationship.

1075

1076 *Trait change over time (Fig. 3 a&b)*

1077 Change over time was modeled at the CRU grid cell (region) level (r), with site (s) as a
1078 random effect when there was more than one site per region (to account for non-
1079 independence of sites within a region) and plot (p) as a random effect for those sites with
1080 permanent (repeating) plots (to account for repeated measures on the same plot over time).
1081 We did not account for temporal autocorrelation as most plots were not measured annually
1082 (average survey interval = 7.2 years) and did not have more than 3 observations over the
1083 study period (average number of survey years per plot = 3.1). Year (y) was centered within
1084 each region.

1085

$$CWMmean_{p,y} \sim Normal(\alpha_p + \alpha_s + \alpha_{r,y}, CWMsd_{p,y})$$

1086

1087 Where $CWMmean_p$ is the mean of the posterior distribution of the community-weighted
1088 mean (CWM) estimate per plot (p) and $CWMsd_p$ is the standard deviation of the posterior
1089 distribution of the CWM estimate per plot, as described in the “*Calculation of CWM values:
1090 incorporating uncertainty in species traits*” section. For non-permanent plots and for sites

1091 that were the only site within a region, α_p or α_s , respectively, were set to 0. Region-level
1092 slopes were then used to fit an average trend of community trait values over time:
1093

$$\begin{aligned}\alpha_{r,y} &\sim \text{Normal}(\alpha_r + \beta_r \cdot \text{year}_{y,r}, \sigma_0) \\ \beta_r &\sim \text{Normal}(B, \sigma_1) \\ \alpha_r &\sim \text{Normal}(A, \sigma_2)\end{aligned}$$

1094

1095 where A and B are the intercept and slope hyperparameters, respectively. See
1096 supplementary information for complete STAN code. This model was used for both
1097 community-weighted mean (CWM) and non-weighted mean plot-level estimates in order to
1098 determine the degree to which temporal trait change is due to species turnover alone (non-
1099 weighted mean) and for CWM+ITV plot-level estimates to determine the potential additional
1100 contribution of intraspecific trait variation to overall trait change.

1101

1102 Standardized effect sizes for CWM change over time (Fig. 3b) were obtained by dividing the
1103 slope of overall trait change over time (mean hyperparameter across 117 sites) by the
1104 standard deviation of the slope estimates per site. Effect sizes for turnover-only and
1105 CWM+ITV change are estimated relative to the CWM change value for that trait based on
1106 the slope values of each.

1107

1108 To estimate change in the proportion of woody and evergreen species over time (CWM
1109 change only; Extended Data Fig. 3 c&d) we used a beta-Bernoulli mixture model of the
1110 same form described above. The discrete and continuous components of the data were
1111 modeled separately, with mixing occurring at the region x year effect ($\alpha_{r,y}$). We additionally
1112 assessed whether the rate of observed trait change over time was related to the duration of
1113 vegetation monitoring at each site. There was no influence of monitoring duration for any
1114 trait (not shown).

1115

1116 *Temperature sensitivity (Fig. 3c)*

1117 Temperature sensitivity was modeled as the variation in CWM trait values with variation in
1118 the five-year mean temperature (i.e., the mean temperature of the survey year and the four
1119 preceding years). A four-year lag was chosen because this interval has been shown to best
1120 explain vegetation change in tundra²⁰ and alpine²⁹ plant communities. The model specifics
1121 are exactly as shown above for “Trait change over time”, but with temperature in the place of
1122 year. Temperatures were centered within each region.

1123

1124 *Observed vs. expected trait change (Fig. 4a)*

1125 We first calculated the mean rate of temperature change across the 38 regions in our study,
1126 and then estimated the *expected* degree of change in each trait over the same period based
1127 on this temperature change and the spatial relationship between temperature and CWM trait
1128 values (described in the “*Spatial community trait models*” section). We then compared this
1129 *expected* trait change to actual trait change over time (described in the “*Trait change over*
1130 *time*” section). To create Fig. 4a we used the overall predicted mean value of each trait in
1131 the first year of survey (1989) as an intercept, and then used the expected and observed
1132 rates of trait change (+/- uncertainty) to predict community trait values in each year
1133 thereafter. We subtracted the intercept from all predicted values in order to show trait
1134 change as an anomaly (difference from 0). The difference between the expected (black) and
1135 observed (colored) lines in Fig. 4a represents a deviation from expected. To calculate total
1136 trait change including the estimated contribution of intraspecific change (colored dashed
1137 lines), we followed the same procedure as described for “observed” trait change but where
1138 this observed change was based on plot-level CWM+ITV estimates that varied by year
1139 based on the temperature in that year and the temperature-trait relationship per species
1140 (described in the “*Calculation of CWM values: partitioning turnover and estimating*
1141 *contribution of ITV*” section).

1142

1143 *Trait change vs. temperature change and soil moisture (Extended Data Fig. 5)*

1144 To determine whether the rate of trait change can be explained by the rate of temperature
1145 change at a site, the (static) level of soil moisture of a site, or their interaction, we modeled
1146 the rate of trait change as described above (“Trait change over time”) and compared it to the
1147 rate of temperature change over the same time interval (with a lag of four years) and soil
1148 moisture:

1149

$$\beta_r \sim \text{Normal}(\gamma_0 + \gamma_1 \cdot \text{temp}_r + \gamma_2 \cdot \text{moisture}_r + \gamma_3 \cdot \text{temp}_r \cdot \text{moisture}_r, \sigma)$$

1150

1151 where β_r is the rate of trait change per region (Extended Data Fig. 5a). When sites within a
1152 region were measured over different intervals or contained different soil moisture estimates
1153 they were modeled separately in order to match with temperature change estimates over the
1154 same interval and soil moisture estimates, which vary at the site level.

1155

1156 We also conducted this analysis using estimates of soil moisture change (with a lag of four
1157 years) from downscaled ERA-Interim (volumetric soil water layer 1). This model took the
1158 same form as above, but with moisture change in place of static soil moisture estimates
1159 (Extended Data Fig. 5b). Trait change was modeled at the site (rather than region) level

1160 because estimates of soil moisture change vary at the site level. Because ERA-Interim data
1161 were not available for every site, this analysis was conducted with a total of 101 rather than
1162 117 sites. We note that the results of this analysis should be interpreted cautiously, as local
1163 changes in soil moisture may not be well represented by coarse-scale remotely sensed data,
1164 as described previously.

1165

1166 *Species gains and losses as a function of traits (Extended Data Fig. 6)*

1167 We estimated species gains and losses at the site (rather than plot) level to reduce the effect
1168 of random fluctuations in species presences/absences due to observer error. Thus, sites
1169 with repeating and non-repeating plots were treated the same. A “gain” was defined as a
1170 species that did not occur in a site in the first survey year but did in the last survey year,
1171 while a “loss” was the reverse. We then modeled the probability of gain or loss separately as
1172 a function of the mean trait value of each species. For example, for “gains,” all newly
1173 observed species received a response type of 1 while all other species in the site received a
1174 response type of 0:

1175

$$response_i \sim \text{Bernoulli}(\alpha_s + \alpha_r + \beta_r \cdot trait_i)$$

$$\alpha_r \sim \text{Normal}(A, \sigma_1)$$

$$\beta_r \sim \text{Normal}(B, \sigma_2)$$

$$\alpha_s \sim \text{Normal}(0, \sigma_r)$$

1176

1177 We included a random effect for site (s) only when there were multiple sites within the same
1178 region (r), otherwise α_s was set to 0. We considered species' responses to be related to a
1179 given trait when the 95% credible interval on the slope hyperparameter (B) did not overlap
1180 zero.

1181

1182 *Trait projections with warming (Extended Data Fig. 7)*

1183 We projected trait change for the minimum (RCP2.6) and maximum (RCP8.5) IPCC carbon
1184 emission scenarios from the NIMR HadGEM2-AO Global Circulation Model. We used the
1185 midpoint years of the WorldClim (1975) and HadGem2 (2090) estimates to calculate the
1186 expected rate of temperature change over this time period. We then predicted trait values for
1187 each year into the future based on the projected rate of temperature change and the spatial
1188 relationship between temperature and community trait values (described in the “*Spatial*
1189 *community trait models*” section).

1190

1191 These projections are not intended to predict actual expected trait change over the next
1192 century, as many other factors not accounted for here will also influence this change. In
1193 particular, future changes in functional traits will likely depend on concurrent changes in
1194 moisture availability, which are less well understood than temperature change. Recent
1195 modeling efforts predict increases in precipitation across much of the Arctic⁵⁷, but it is
1196 unknown whether increasing precipitation will also lead to an increase in soil moisture/water
1197 availability for plants, as the drying effect of warmer temperatures (e.g. due to increased
1198 evaporation and/or decreased duration of snow cover⁵⁸) may outweigh the impact of
1199 increased precipitation. Instead, these projections are an attempt to explore theoretical trait
1200 change over the long-term when using a space-for-time substitution approach.

1201

1202 *Principal component analysis (PCA; Extended Data Fig. 8)*

1203 We performed an ordination of community-weighted trait mean values per plot on all seven
1204 traits. Because community evergreenness could only be estimated for plots with at least one
1205 woody species, the total number of plots included in this analysis is reduced compared to
1206 the entire dataset (1098 plots out of 1520 in total). We used the R package *vegan*⁵⁹ (v. 2.4.6)
1207 to conduct a principal component analysis of these data. This analysis uses only trait means
1208 per plot, and therefore information about CWM uncertainty due to intraspecific trait variation
1209 and/or missing species is lost. The analysis was performed on log-transformed trait values⁴⁹.
1210 We extracted the axis coordinates of each plot from the PCA and used the spatial trait-
1211 temperature-moisture model described above (section “*Spatial community trait models*”) to
1212 determine whether plot positions along both PCA axes varied with temperature, moisture,
1213 and their interaction.

1214

1215 *Trends in species abundance (Supplementary Information, Table S10)*

1216 In order to provide more insight into the species-specific changes occurring over time in
1217 tundra ecosystems, we calculated trends in abundance for the most common (widespread
1218 and abundant) species in the community composition dataset. We estimated trends for all
1219 species that occurred in at least 5 sites at a minimum abundance of 5% cover (mean of all
1220 plots within a site) across all years. We additionally included species that occurred at low
1221 abundance (1% or more) but were widespread (at least 10 sites). This technique yielded a
1222 total of 79 species. Abundance changes were modeled as described for trait change over
1223 time, but because abundance (proportion of plot cover) is bounded between 0 and 1,
1224 inclusive, we used a beta-Bernoulli mixture model. Abundance change was then estimated
1225 per species (*sp*) across all regions (*r*):

1226

$$\alpha_{sp,r,y} \sim \text{Normal}(\alpha_{sp,r} + \beta_{sp,r} \cdot \text{year}_{sp,r,y}, \sigma_{sp})$$

$$\beta_{sp,r} \sim Normal(B_{sp}, \sigma_1)$$

$$\alpha_{sp,r} \sim Normal(A_{sp}, \sigma_2)$$

1227

1228 We additionally extracted region-specific slopes per species ($\beta_{sp,r}$) in order to calculate a
1229 proportion of regions in which a given species was increasing or decreasing (“Prop.
1230 Increase” and “Prop. Decrease” in Table S10). Because regional slopes are modeled as
1231 random effects, these estimates are not entirely independent (i.e., they will be pulled toward
1232 the overall species mean slope), but provide an approximate estimate of whether directional
1233 trends in abundance are consistent across a species’ range.

1234

1235 **Methods References**

- 1236 41. Harris, I., Jones, P. D., Osborn, T. J. & Lister, D. H. Updated high-resolution grids of
1237 monthly climatic observations – the CRU TS3.10 Dataset. *International Journal of*
1238 *Climatology* **34**, 623–642 (2014).
- 1239 42. Blok, D. *et al.* The Cooling Capacity of Mosses: Controls on Water and Energy Fluxes
1240 in a Siberian Tundra Site. *Ecosystems* **14**, 1055–1065 (2011).
- 1241 43. Soudzilovskaia, N. A., van Bodegom, P. M. & Cornelissen, J. H. C. Dominant
1242 bryophyte control over high-latitude soil temperature fluctuations predicted by heat
1243 transfer traits, field moisture regime and laws of thermal insulation. *Functional Ecology*
1244 **27**, 1442–1454 (2013).
- 1245 44. Hijmans, R. J., Cameron, S. E., Parra, J. L., Jones, J. L. & Jarvis, A. Very high
1246 resolution interpolated climate surfaces for global land areas. *International Journal of*
1247 *Climatology* **25**, 1965–1978 (2005).
- 1248 45. Myers-Smith, I. H. *et al.* Climate sensitivity of shrub growth across the tundra biome.
1249 *Nature Climate Change* **5**, 887–891 (2015).
- 1250 46. Willmott, C. J. & Robeson, S. M. Climatologically aided interpolation (CAI) of terrestrial
1251 air temperature. *International Journal of Climatology* **15**, 221–229 (1995).
- 1252 47. Sperna Weiland, F. C., Vrugt, J. A., van Beek, R. L.). P. H., Weerts, A. H. & Bierkens,
1253 M. F. P. Significant uncertainty in global scale hydrological modeling from precipitation
1254 data errors. *Journal of Hydrology* **529**, 1095–1115 (2015).
- 1255 48. Beguería, S., Vicente Serrano, S. M., Tomás Burguera, M. & Maneta, M. Bias in the
1256 variance of gridded data sets leads to misleading conclusions about changes in climate
1257 variability. *International Journal of Climatology* **36**, 3413–3422 (2016).
- 1258 49. Kattge, J. *et al.* TRY—a global database of plant traits. *Global Change Biology* **17**,
1259 2905–2935 (2011).
- 1260 50. Bjorkman, A. D. *et al.* Tundra Trait Team: A database of plant traits spanning the
1261 tundra biome. *Global Ecology and Biogeography*
- 1262 51. Cayuela, L., Granzow-de la Cerda, Í., Albuquerque, F. S. & Golicher, D. J.
1263 TAXONSTAND: An R package for species names standardisation in vegetation
1264 databases. *Methods in Ecology and Evolution* **3**, 1078–1083 (2012).
- 1265 52. Plummer, M. rjags: Bayesian graphical models using MCMC. (2016).
- 1266 53. Stan Development Team. RStan: the R interface to Stan. (2016).
- 1267 54. Gelman, A. & Rubin, D. B. Inference from iterative simulation using multiple
1268 sequences. *Statistical Science* **7**, 457–472 (1992).
- 1269 55. Messier, J., McGill, B. J. & Lechowicz, M. J. How do traits vary across ecological
1270 scales? A case for trait-based ecology. *Ecology Letters* **13**, 838–848 (2010).

- 1271 56. Violle, C. *et al.* The return of the variance: intraspecific variability in community
1272 ecology. *Trends Ecol. Evol.* **27**, 245–253 (2012).
- 1273 57. Bintanja, R. & Selten, F. M. Future increases in Arctic precipitation linked to local
1274 evaporation and sea-ice retreat. *Nature* **509**, 479–482 (2014).
- 1275 58. AMAP. *Snow, Water, Ice and Permafrost in the Arctic (SWIPA) 2017*. (Arctic
1276 Monitoring and Assessment Programme (AMAP), 2017).
- 1277 59. Oksanen, J., Blanchet, F., Kindt, R. & Legendre, P. Package ‘vegan’. (2011).
- 1278 60. Chapin, F. S., III, BretHarte, M. S., Hobbie, S. E. & Zhong, H. L. Plant functional types
1279 as predictors of transient responses of arctic vegetation to global change. *Journal of*
1280 *Vegetation Science* **7**, 347–358 (1996).
- 1281 61. Weiher, E. *et al.* Challenging Theophrastus: A Common Core List of Plant Traits for
1282 Functional Ecology. *Journal of Vegetation Science* **10**, 609–620 (1999).
- 1283 62. Violle, C. *et al.* Let the concept of trait be functional! *Oikos* **116**, 882–892 (2007).
- 1284 63. Hudson, J. M. G. & Henry, G. H. R. Increased plant biomass in a High Arctic heath
1285 community from 1981 to 2008. *Ecology* **90**, 2657–2663 (2009).
- 1286 64. De Deyn, G. B., Cornelissen, J. H. C. & Bardgett, R. D. Plant functional traits and soil
1287 carbon sequestration in contrasting biomes. *Ecology Letters* **11**, 516–531 (2008).
- 1288 65. Kunstler, G. *et al.* Plant functional traits have globally consistent effects on competition.
1289 *Nature* **529**, 204–207 (2016).
- 1290 66. Gaudet, C. L. & Keddy, P. A. A Comparative Approach to Predicting Competitive Ability
1291 From Plant Traits. *Nature* **334**, 242–243 (1988).
- 1292 67. Westoby, M., Falster, D. S., Moldes, A. T., Vesk, P. A. & WRIGHT, I. J. Plant
1293 ecological strategies: Some leading dimensions of variation between species. *Annual*
1294 *Review of Ecology and Systematics* **33**, 125–159 (2002).
- 1295 68. Moles, A. T. & Leishman, M. R. *Seedling Ecology and Evolution*. (Cambridge
1296 University Press, 2008).
- 1297 69. Sturm, M. *et al.* Snow-shrub interactions in Arctic tundra: a hypothesis with climatic
1298 implications. *Journal of Climate* **14**, 336–344 (2001).
- 1299 70. Lorant, M. M., Berner, L. T., Goetz, S. J., Jin, Y. & Randerson, J. T. Vegetation
1300 controls on northern high latitude snow-albedo feedback: observations and CMIP5
1301 model simulations. *Global Change Biology* **20**, 594–606 (2014).
- 1302 71. Myers-Smith, I. H. & Hik, D. S. Shrub canopies influence soil temperatures but not
1303 nutrient dynamics: An experimental test of tundra snow-shrub interactions. *Ecol Evol* **3**,
1304 3683–3700 (2013).
- 1305 72. DeMarco, J., Mack, M. C. & Bret-Harte, M. S. Effects of arctic shrub expansion on
1306 biophysical vs. biogeochemical drivers of litter decomposition. *Ecology* **95**, 1861–1875
1307 (2014).

- 1308 73. Enquist, B. J., Brown, J. H. & West, G. B. Allometric scaling of plant energetics and
1309 population density. *Nature* **395**, 163–165 (1998).
- 1310 74. Street, L. E., Shaver, G. R., Williams, M. & van Wijk, M. T. What is the relationship
1311 between changes in canopy leaf area and changes in photosynthetic CO₂ flux in arctic
1312 ecosystems? *Journal of Ecology* **95**, 139–150 (2007).
- 1313 75. Poorter, H. *et al.* Biomass allocation to leaves, stems and roots: meta-analyses of
1314 interspecific variation and environmental control. *New Phytol.* **193**, 30–50 (2012).
- 1315 76. Greaves, H. E. *et al.* Estimating aboveground biomass and leaf area of low-stature
1316 Arctic shrubs with terrestrial LiDAR. *Remote Sensing of Environment* **164**, 26–35
1317 (2015).
- 1318 77. Westoby, M. & Wright, I. J. Land-plant ecology on the basis of functional traits. *Trends*
1319 *Ecol. Evol.* **21**, 261–268 (2006).
- 1320 78. Niinemets, Ü. A review of light interception in plant stands from leaf to canopy in
1321 different plant functional types and in species with varying shade tolerance. *Ecological*
1322 *Research* **25**, 693–714 (2010).
- 1323 79. Freschet, G. T., Aerts, R. & Cornelissen, J. H. C. A plant economics spectrum of litter
1324 decomposability. *Functional Ecology* **26**, 56–65 (2012).
- 1325 80. Manning, P. *et al.* Simple measures of climate, soil properties and plant traits predict
1326 national-scale grassland soil carbon stocks. *Journal of Applied Ecology* **52**, 1188–1196
1327 (2015).
- 1328 81. Lida, Y. *et al.* Wood density explains architectural differentiation across 145 co-
1329 occurring tropical tree species. *Functional Ecology* **26**, 274–282 (2012).
- 1330 82. Ménard, C. B., Essery, R., Pomeroy, J., Marsh, P. & Clark, D. B. A shrub bending
1331 model to calculate the albedo of shrub-tundra. *Hydrological Processes* **28**, 341–351
1332 (2014).
- 1333 83. Nauta, A. L. *et al.* Permafrost collapse after shrub removal shifts tundra ecosystem to a
1334 methane source. *Nature Climate Change* **5**, 67–70 (2015).
- 1335 84. Hobbie, S. E. Temperature and Plant Species Control Over Litter Decomposition in
1336 Alaskan Tundra. *Ecological Monographs* **66**, 503–522 (1996).
- 1337 85. Weedon, J. T. *et al.* Global meta-analysis of wood decomposition rates: a role for trait
1338 variation among tree species? *Ecology Letters* **12**, 45–56 (2009).
- 1339 86. Dorrepaal, E., Cornelissen, J., Aerts, R., Wallen, B. & Van Logtestijn, R. Are growth
1340 forms consistent predictors of leaf litter quality and decomposability across peatlands
1341 along a latitudinal gradient? *Journal of Ecology* **93**, 817–828 (2005).
- 1342 87. Larsen, K. S., Michelsen, A., Jonasson, S., Beier, C. & Grogan, P. Nitrogen Uptake
1343 During Fall, Winter and Spring Differs Among Plant Functional Groups in a Subarctic
1344 Heath Ecosystem. *Ecosystems* **15**, 927–939 (2012).

- 1345 88. Chapin, F. S., III, Shaver, G. R., Giblin, A. E., Nadelhoffer, K. J. & Laundre, J. A.
1346 Responses of arctic tundra to experimental and observed changes in climate. *Ecology*
1347 **76**, 694–711 (1995).
- 1348 89. Reich, P. B., Walters, M. B. & Ellsworth, D. S. From tropics to tundra: Global
1349 convergence in plant functioning. *Proceedings of the National Academy of Sciences*
1350 **94**, 13730–13734 (1997).
- 1351 90. Dornelas, M. *et al.* BioTIME: A database of biodiversity time series for the
1352 Anthropocene. *Global Ecology and Biogeography* **27**, 760–786 (2018).
1353

1354 **DATA AVAILABILITY**

1355

1356 *Trait data*

1357 Data compiled through the Tundra Trait Team are publicly accessible⁵⁰ (data paper
1358 published in *Global Ecology & Biogeography*). The public TTT database includes traits not
1359 considered in this study as well as tundra species that do not occur in our vegetation survey
1360 plots, for a total of nearly 92,000 trait observations on 978 species. Additional trait data from
1361 the TRY trait database can be requested at try-db.org.

1362

1363 *Composition data*

1364 Most sites and years of the vegetation survey data included in this study are available in the
1365 Polar Data Catalogue (ID # 10786_iso). Much of the individual site-level data has
1366 additionally been made available in the BioTIME database⁹⁰ ([https://synergy.st-
1367 andrews.ac.uk/biotime/biotime-database/](https://synergy.st-andrews.ac.uk/biotime/biotime-database/)).

1368

1369 *References*

1370 50. Bjorkman, AD, IH Myers-Smith, SC Elmendorf, S Normand, HJD Thomas, *et al.* Tundra
1371 Trait Team: a database of plant traits spanning the tundra biome. *Global Ecology and*
1372 *Biogeography*. *In press*.

1373 90. Dornelas, M, LH Antão, F Moyes, AE Bates, AE Magurran, *et al.* 2018. BioTIME: A
1374 database of biodiversity time series for the Anthropocene. *Global Ecology and*
1375 *Biogeography*. 27: 760-786.

1376

1377 **CODE AVAILABILITY**

1378

1379 STAN code for the two main models (spatial temperature-moisture-trait relationships and
1380 community trait change over time) is provided in the Supplementary Information associated
1381 with this study (available online).

1382 **Extended Data Fig. 1. Overview of trait data and analyses. a**, Count of traits per latitude
1383 (rounded to the nearest degree) for all georeferenced observations in TRY and TTT that
1384 correspond to species in the vegetation survey dataset. **b**, Work flow and analyses of
1385 temperature-trait relationships. Intraspecific temperature-trait relationships over space were used to
1386 estimate the potential contribution of ITV to overall temperature-trait relationships over space and time
1387 (CWM + ITV) as trait measurements on individuals over time are not available.

1388

1389 **Extended Data Fig. 2. All temperature-trait relationships.** Slope of temperature-trait
1390 relationship over space (within-species (ITV) and across communities (CWM)) and with
1391 interannual variation in temperature (community temperature sensitivity). Spatial – ITV is the
1392 average intraspecific trait variation as related to temperature over space, Spatial – CWM is
1393 the relationship between community-weighted trait means and summer temperature, and
1394 Temporal sensitivity – CWM is the temperature sensitivity of community-weighted trait
1395 means (i.e., correspondence between interannual variation in CWM values with interannual
1396 variation in temperature). Error bars represent 95% credible intervals on the slope estimate.
1397 We used five-year mean temperatures (temperature of the survey year and four previous
1398 years) to estimate temperature sensitivity because this interval has been shown to explain
1399 vegetation change in tundra²⁰ and alpine²⁹ plant communities. All slope estimates are in
1400 transformed units (height = log cm, LDMC = logit g/g, leaf area = log cm², leaf nitrogen = log
1401 mg/g, SLA = log mm²/mg). Community (CWM) temperature-trait relationships are estimated
1402 across all 117 sites; intraspecific temperature-trait relationships are estimated as the mean
1403 of 108-109 species for SLA, 80-86 species for plant height, 74-72 species for leaf nitrogen,
1404 85-76 species for leaf area, and 43-52 species for LDMC, for summer and winter
1405 temperature, respectively (see *Methods: Analyses: Intraspecific Trait Variation* for details).

1406

1407 **Extended Data Fig. 3. Community woodiness and evergreenness over space and time.**
1408 **a-b**, Variation in community woodiness (**a**) and evergreenness (**b**) across space with
1409 summer temperature and soil moisture. Community woodiness is the abundance-weighted
1410 proportion of woody species versus all other plant species in the community. Community
1411 evergreenness is the abundance-weighted proportion of evergreen shrubs versus all shrub
1412 species (deciduous and evergreen). The evergreen model was conducted on a reduced
1413 number of sites (98 instead of 117) because some sites did not have any woody species
1414 (and it was thus not possible to calculate a proportion evergreen). Both temperature and
1415 moisture were important predictors of community woodiness and evergreenness. The 95%
1416 credible interval for a temperature * moisture interaction term overlapped zero in both
1417 models (-0.100 to 0.114 and -0.201 to 0.069 for woodiness and evergreenness,
1418 respectively). **c-d**, There was no change over time in woodiness (**c**) or evergreenness (**d**).

1419 Thin lines represent slopes per site (woodiness: n = 117 sites, evergreenness, n = 98 sites).
1420 In all panels, bold lines indicate overall model predictions and shaded ribbons designate
1421 95% credible intervals on these model predictions.

1422

1423 **Extended Data Fig. 4. Range in species mean values of each trait by summer**
1424 **temperature.** Black dashed lines represent quantile regression estimates for 1% and 99%
1425 quantiles. Species mean values are estimated from intercept-only Bayesian models using
1426 the estimation technique described in *Methods: Analyses: Calculation of community*
1427 *weighted mean (CWM) values*. Species locations are based on species in the 117
1428 vegetation survey sites. All values are back-transformed into their original units (height = cm,
1429 LDMC = g/g, leaf area = cm², leaf nitrogen = mg/g, SLA = mm²/mg).

1430

1431 **Extended Data Fig. 5. The rate of community trait change is not related to the rate of**
1432 **temperature change or soil moisture for any trait. a-b,** Rate of community-weighted
1433 mean change over time per site (N = 117 sites) as related to temperature change and long-
1434 term mean soil moisture (a) or soil moisture change (b) at a site. Points represent mean trait
1435 change values for each site, lines represent the predicted relationship between trait change,
1436 temperature change and soil moisture/soil moisture change, and transparent ribbons are the
1437 95% CI's on these predictions. Both mean soil moisture and soil moisture change were
1438 modeled as a continuous variables, but are shown as predictions for minimum and
1439 maximum values/rates of change. Trait change estimates are in transformed units (log for
1440 height, leaf area, leaf nitrogen, and SLA, and logit for LDMC). Soil moisture change was
1441 estimated from downscaled ERA Interim data and may not accurately represent local
1442 changes in moisture availability at each site.

1443

1444 **Extended Data Fig. 6. Increasing community height is driven by the immigration of**
1445 **taller species, not the loss of shorter ones.** Probability that a species newly arrived in a
1446 site ("gained") or disappeared from a site ("lost") as a function of its traits (N = 117 sites).
1447 Lines and ribbons represent overall model predictions and the 95% credible intervals on
1448 these predictions, respectively. Dark ribbons and solid lines represent species gains while
1449 pale ribbons and dashed lines represent species losses. Only for plant height was the trait-
1450 probability relationship different for gains and losses.

1451

1452 **Extended Data Fig. 7. Comparison of actual (colored lines), expected (solid black**
1453 **lines), and projected (dotted/dashed black lines) CWM trait change over time.**
1454 Expected trait change is calculated using the observed spatial temperature-trait relationship
1455 and the average rate of recent summer warming across all sites. Note that these projections

1456 assume no change in soil moisture conditions. The dotted/dashed black lines after 2015
1457 show the projected trait change for the maximum (8.5) and minimum (2.6) IPCC carbon
1458 emission scenarios, respectively, from the HadGEM2 AO Global Circulation Model given the
1459 expected temperature change associated with those scenarios. Points along the left axis of
1460 each panel show the distribution of present-day community-weighted trait means per site (N
1461 = 117 sites) to better demonstrate the magnitude of projected change. Values are in original
1462 units (height = cm, LDMC = g/g, leaf area = cm², leaf nitrogen = mg/g, SLA = mm²/mg).

1463

1464 **Extended Data Fig. 8. Community trait co-variation is structured by temperature and**
1465 **moisture. a**, Principal component analysis of plot-level community-weighted traits for seven
1466 key functional traits demonstrating how communities vary in multidimensional trait space.
1467 Trait correlations are highest between SLA and leaf nitrogen, and evergreenness and
1468 woodiness. Variation in SLA, leaf nitrogen, evergreenness and woodiness (PC1) are
1469 orthogonal to variation in height (PC2). Variation in leaf area and LDMC are explained by
1470 both PC 1 and 2. The color of the points indicates the soil moisture status of each plot at the
1471 site-level. **b-c**, Plot scores along PC axis 1, related to plant resource economy, vary with
1472 summer temperature, soil moisture, and their interaction (**b**) while plot scores along PC axis
1473 2 vary only with soil moisture (**c**). The color of the points indicates the soil moisture of each
1474 site. Because not all plots and sites had woody species (and thus proportion evergreen
1475 could not be calculated) this analysis was conducted on a subset of 1098 (out of 1520) plots
1476 in 98 (out of 117) different sites.

1477

1478 **Extended Data Figure 9. Temperature–trait relationships by growth form and site**
1479 **elevation. a**, Mean (+/- SD) intraspecific temperature-height relationships (N = 80 species)
1480 per functional group. Dwarf shrubs are defined as those that do not grow above 30 cm in
1481 height (as estimated by regional floras: Flora of North America, USDA, Royal Horticultural
1482 Society, etc.) and are generally genetically limited in their ability to grow upright. There are
1483 no differences among functional groups in the magnitude of mean intraspecific temperature-
1484 height relationships. **b**, Relationship between community-weighted trait values, summer
1485 temperature, and soil moisture across biogeographic gradients, as in Fig. 2a. Points
1486 represent mean estimates per site (N = 117 sites) and are sized by the elevation of the site
1487 (larger circles = higher elevation). Ribbons represent the overall trait-temperature-moisture
1488 relationship (95% credible intervals on predictions at minimum and maximum soil moisture)
1489 across all sites.

1490

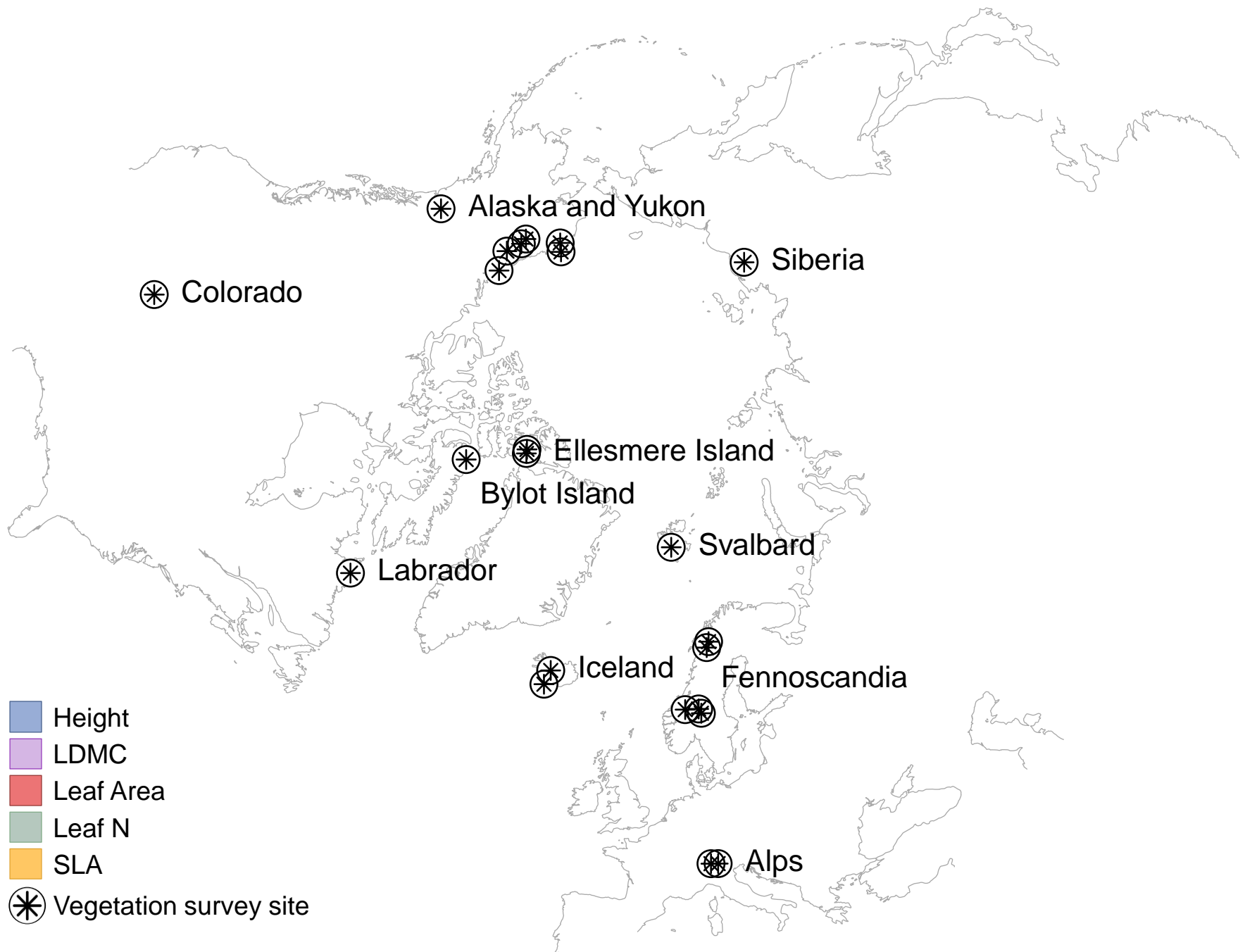
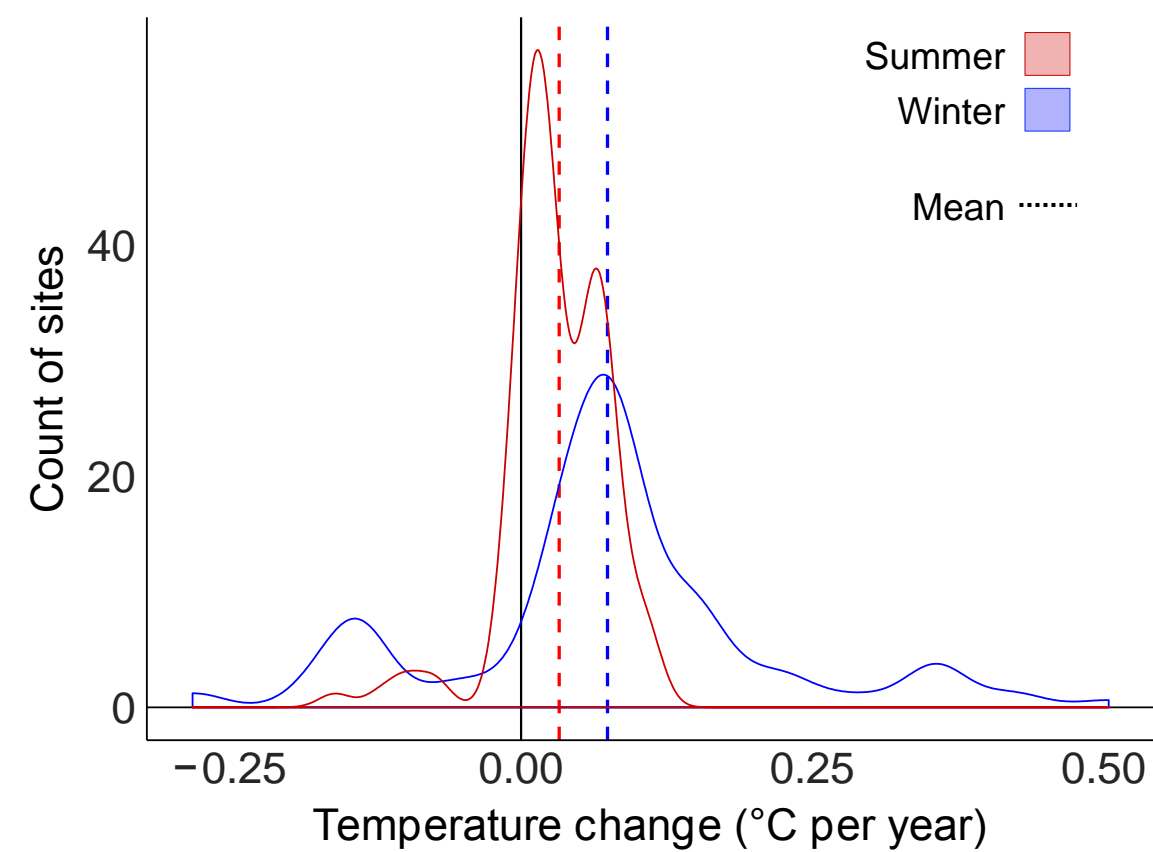
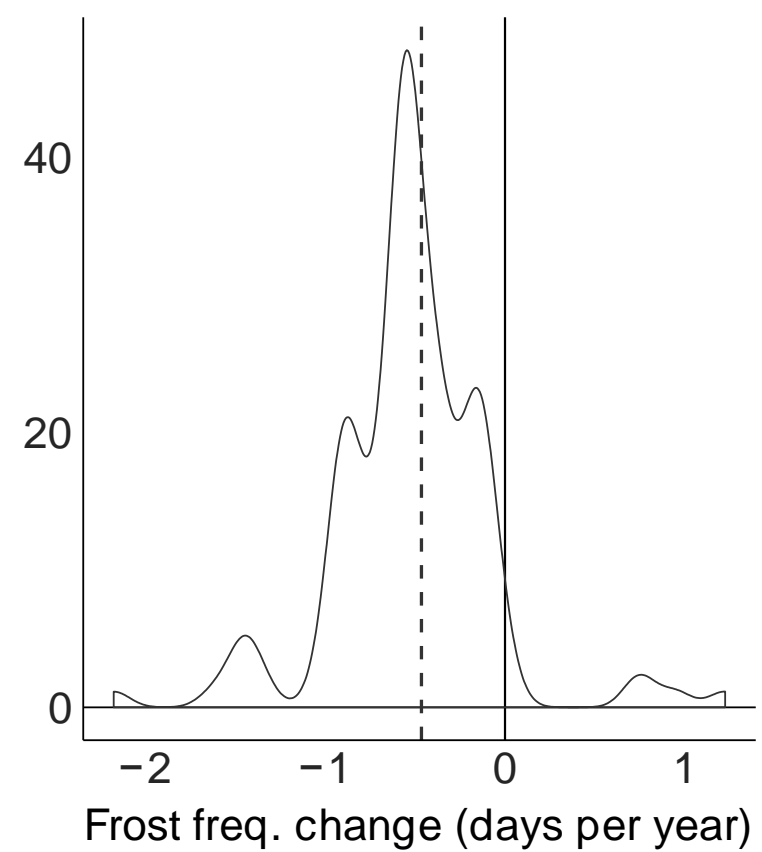
1491 **Extended Data Table 1. Ecosystem functions influenced by each of the seven plant**
1492 **traits investigated.**

A note about all figures:

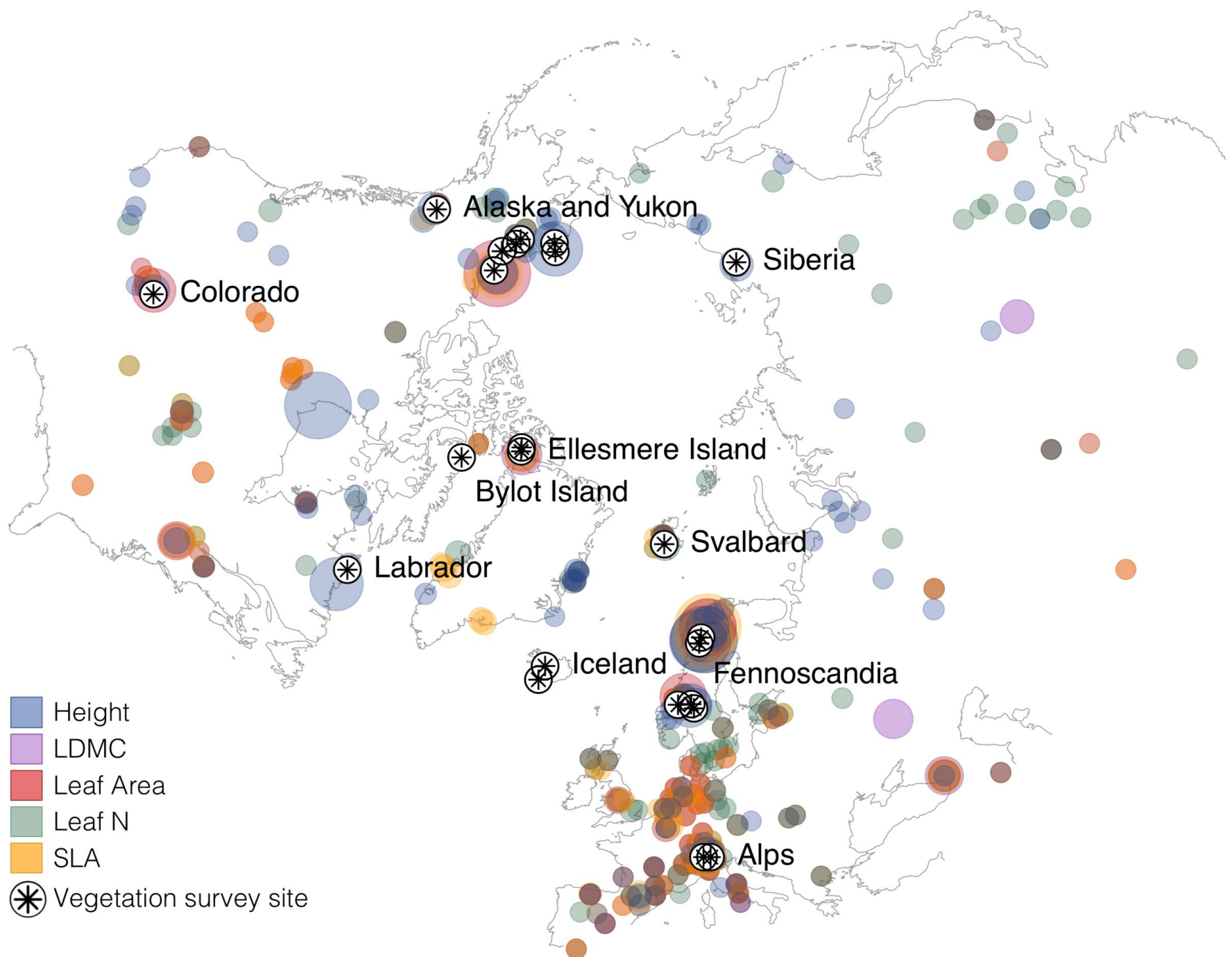
Some of the transparencies (alpha channels in R) in the figures seem to get lost in the conversion from PowerPoint to pdf online, and sometimes also in Mac to PC translation. I have therefore provided a second page in every PowerPoint file that is a screenshot (png) of the way the figure is supposed to look. For example, all the line graphs should have partially transparent ribbons around them. The map (Fig. 1) should have lots of semi-transparent colored dots on it.

I tried exporting with `cairo_pdf` and a number of other things, but was never able to solve the issue. Please let me know if you can recommend an alternative, or if you'd like me to provide alternate files or the R code + data input for making the graphs from scratch.

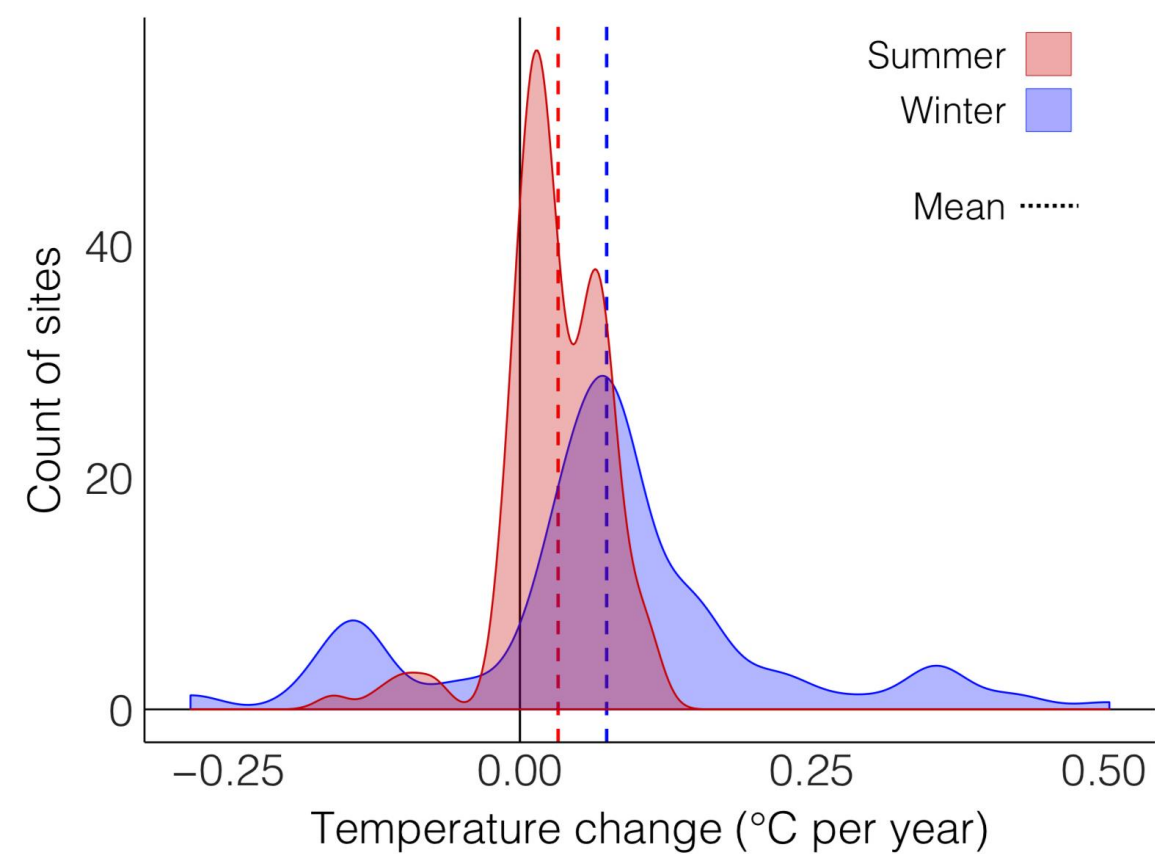
The font used in all figures is Helvetica Light.

a**b** Temperature change**c** Frost frequency change

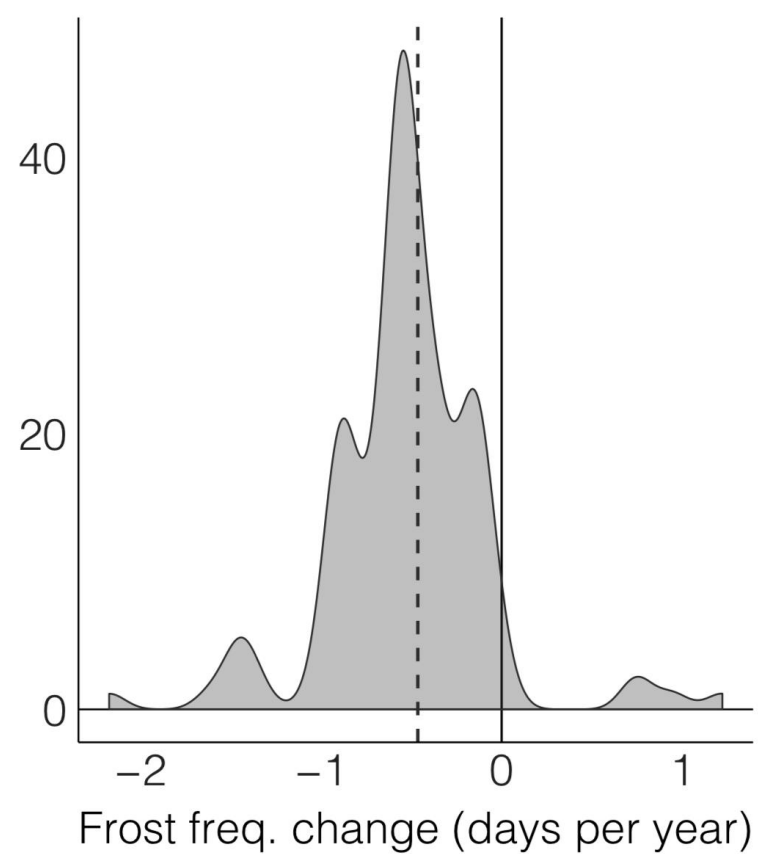
a



b Temperature change

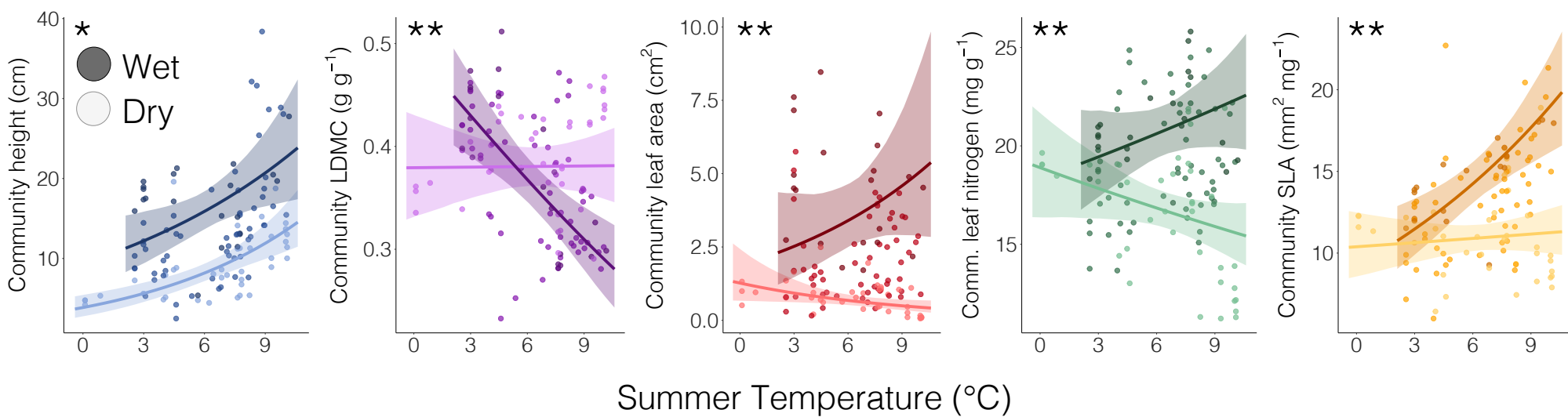


c Frost frequency change

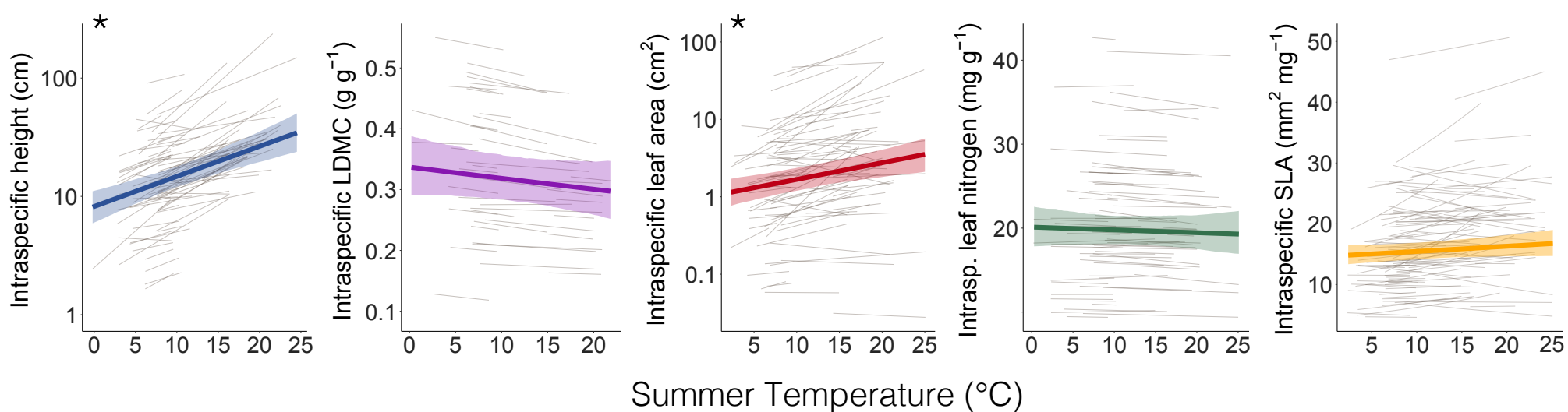


FOR DEMONSTRATION ONLY: THIS IS WHAT IT SHOULD LOOK LIKE (with transparencies)

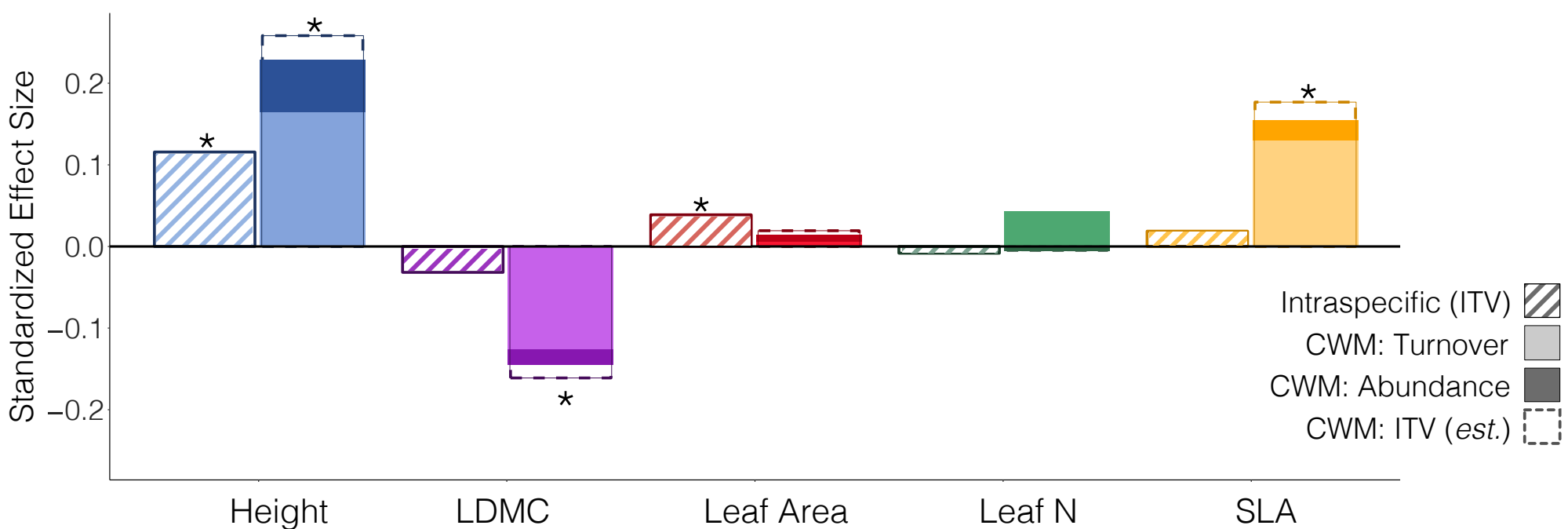
a Temperature – trait relationship: across communities (CWM)



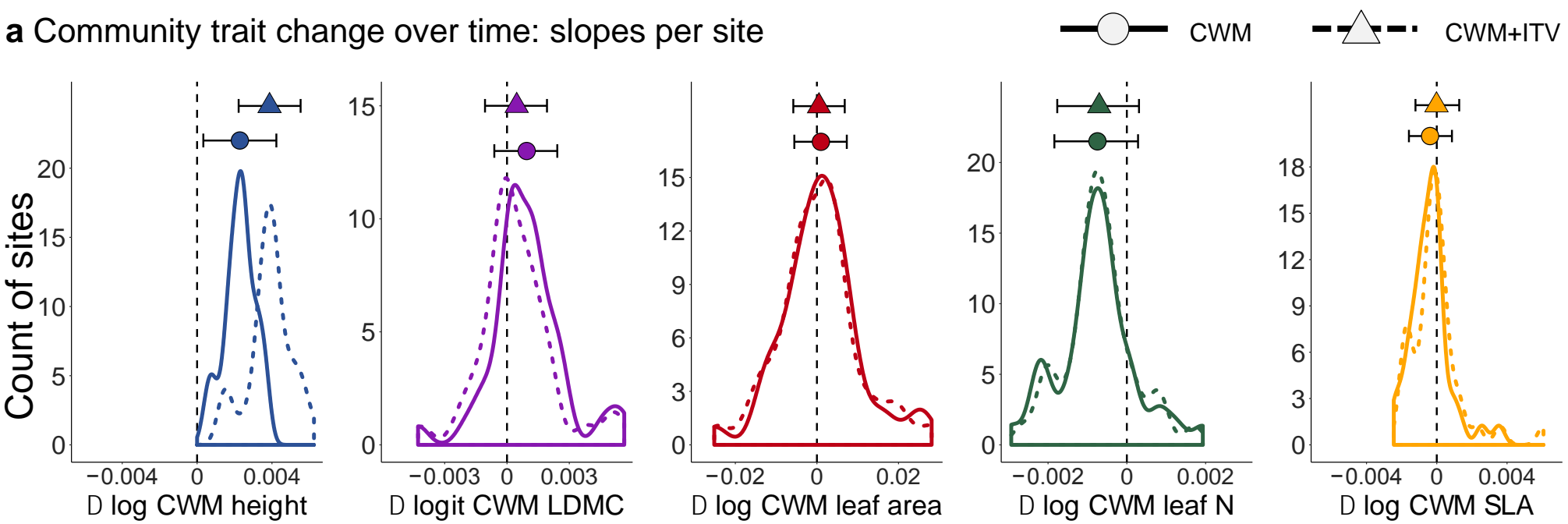
b Temperature – trait relationship: intraspecific trait variation (ITV)



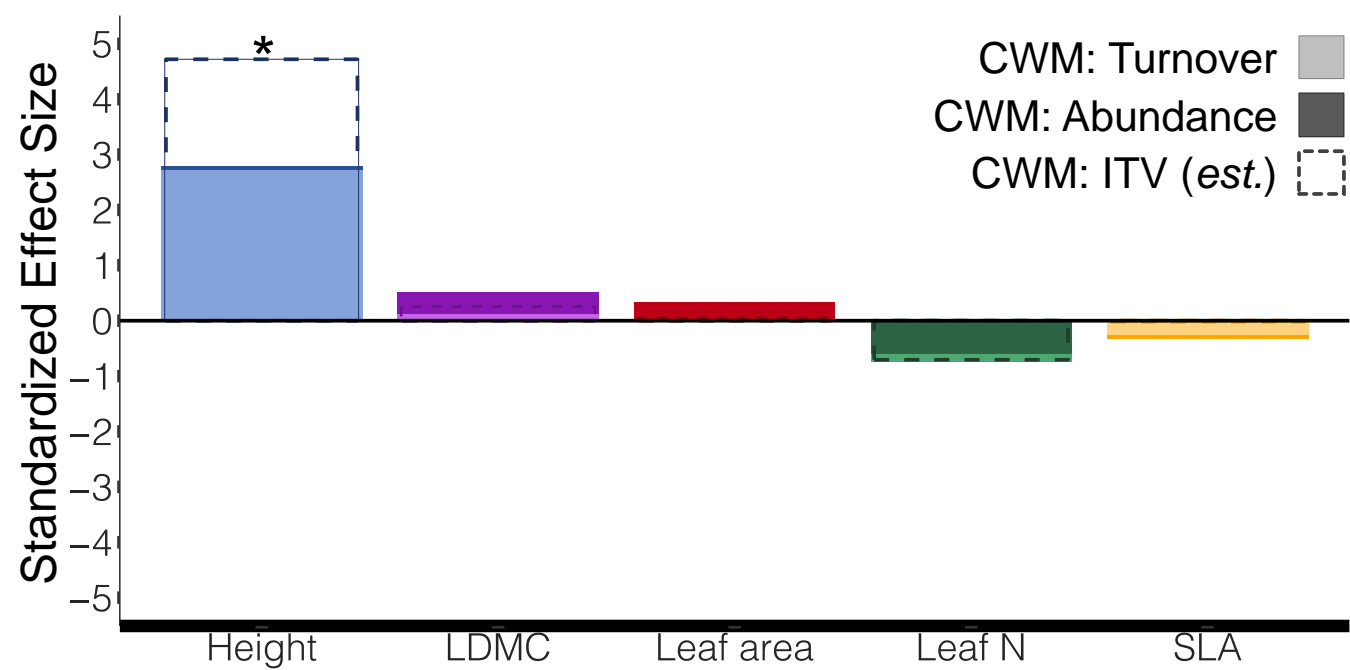
c Temperature – trait relationship: standardized effect size



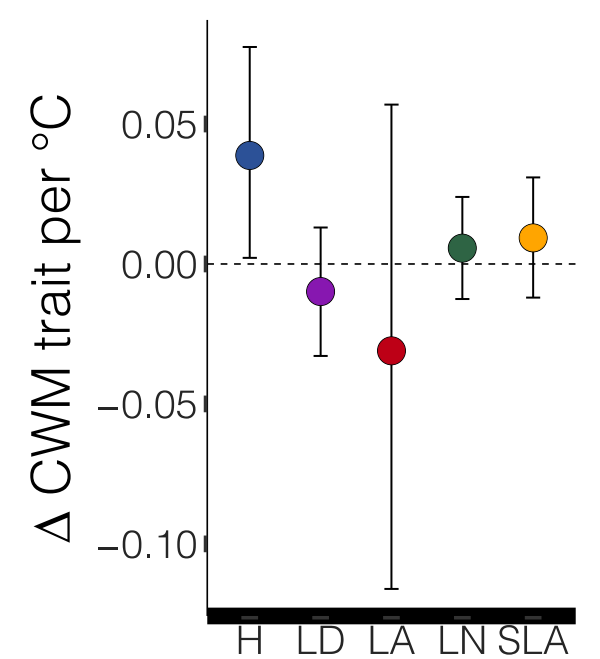
a Community trait change over time: slopes per site

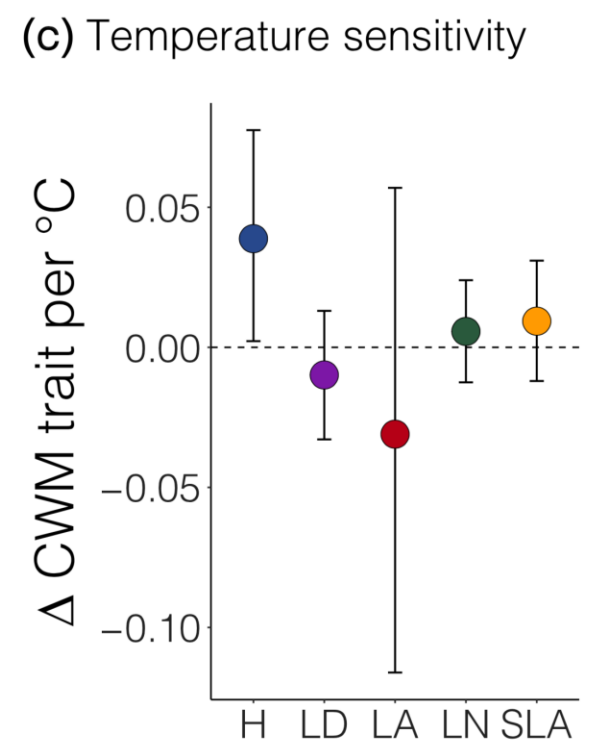
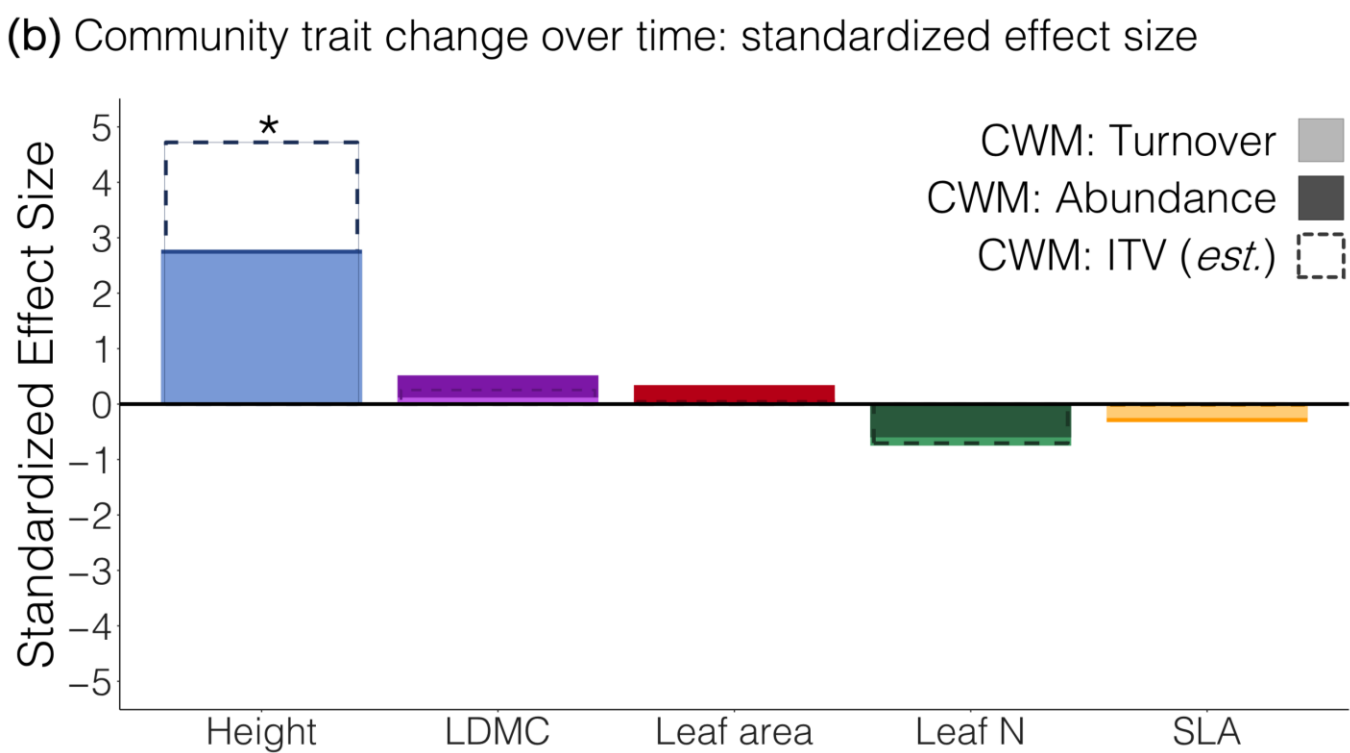
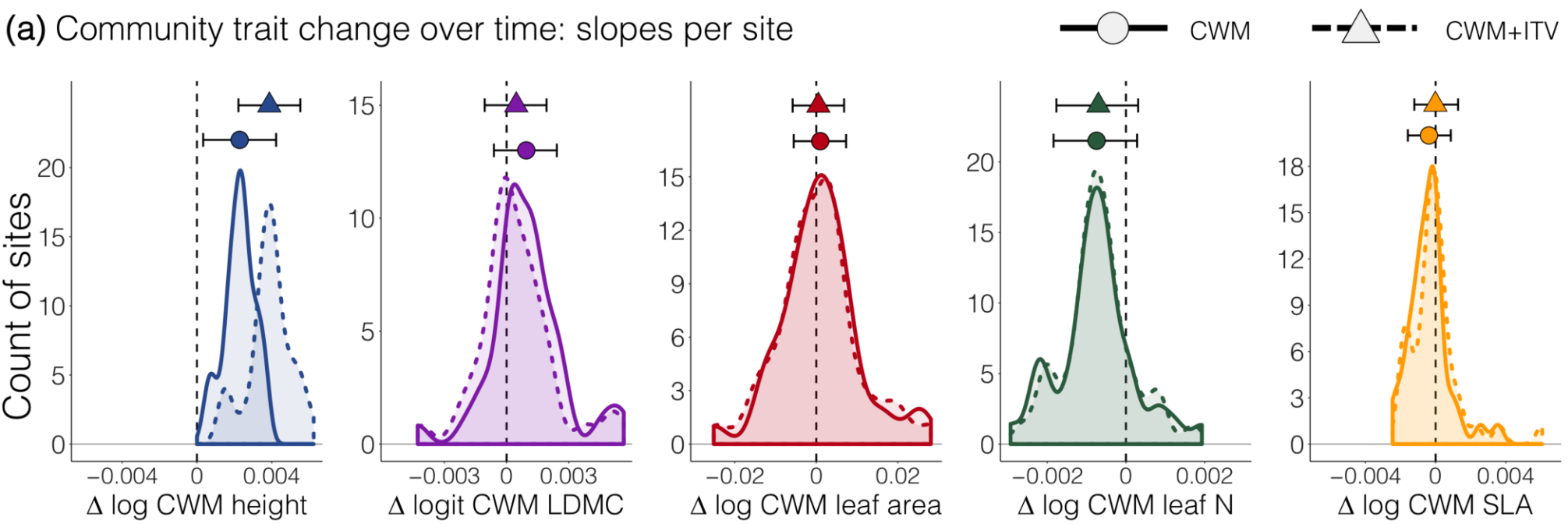


b Community trait change over time: standardized effect size

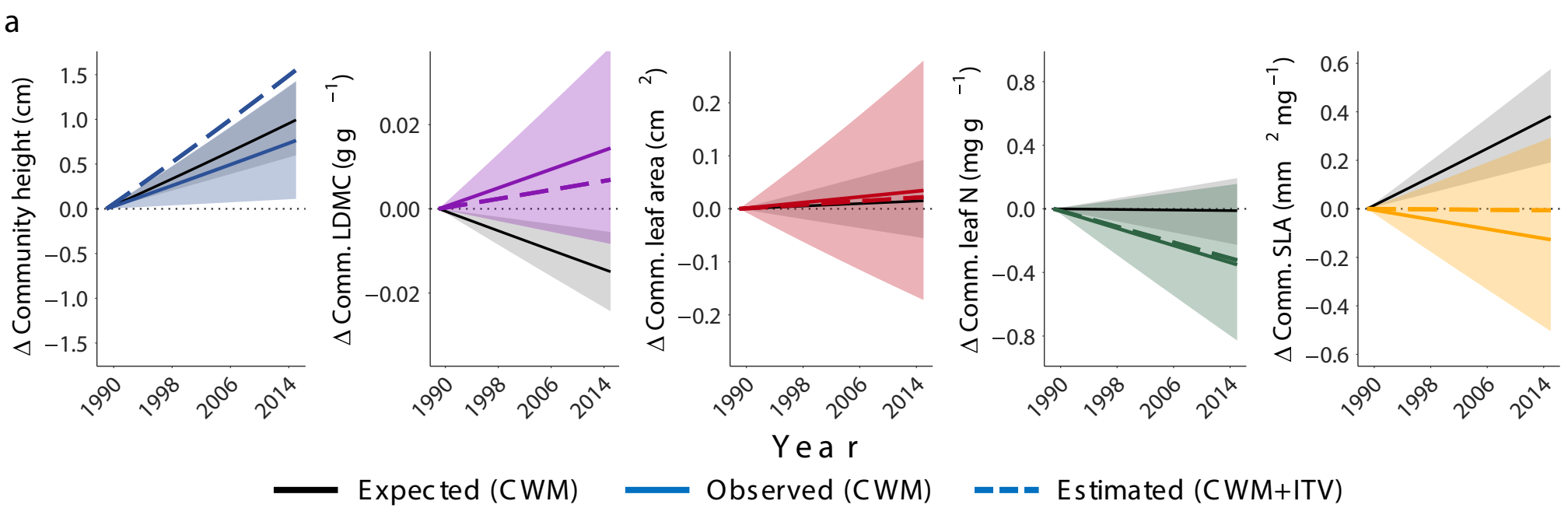


c Temperature sensitivity

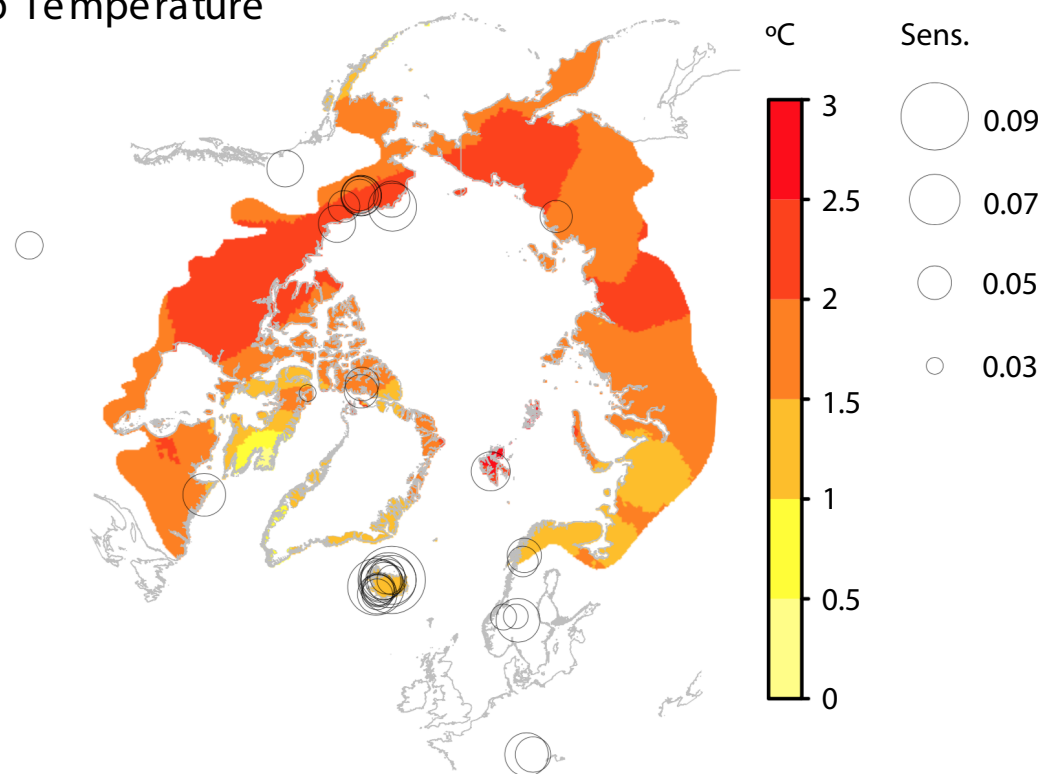




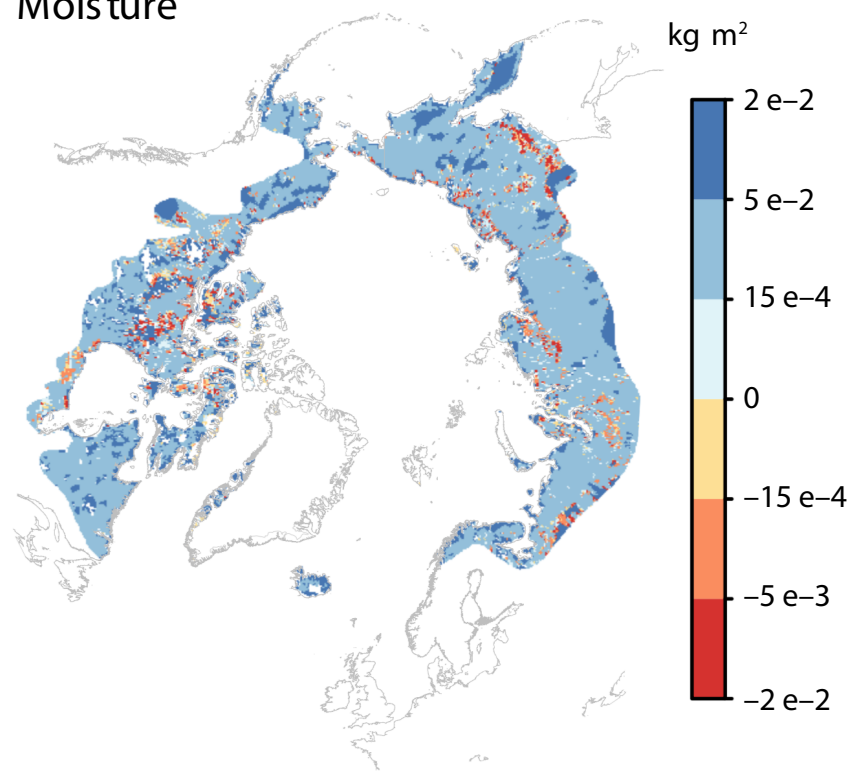
THIS IS WHAT IT SHOULD LOOK LIKE (with transparencies)



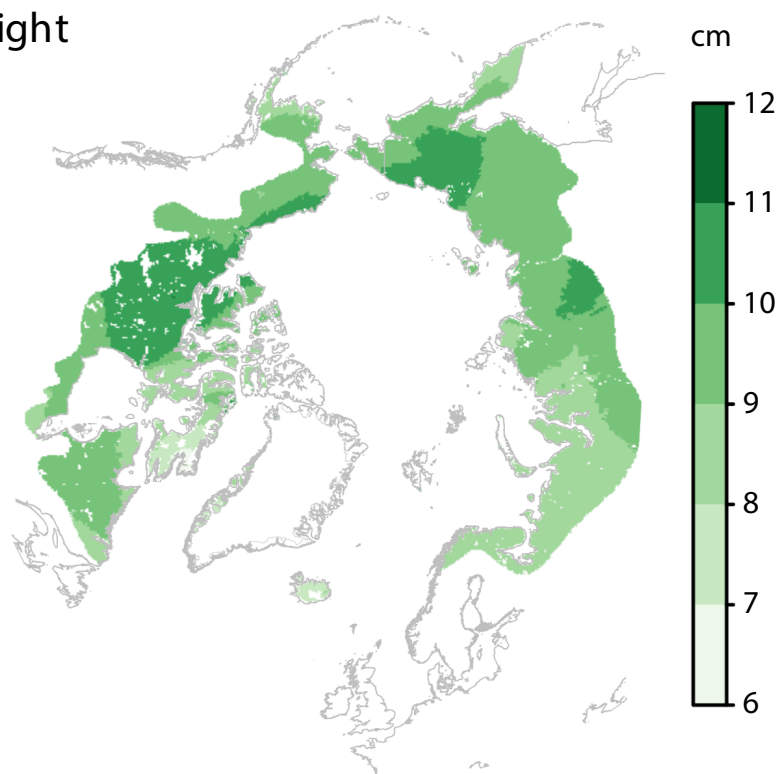
b Temperature



c Moisture



d Height



e Leaf N

